Chapter 5

Mathematical modelling of trace element dynamics in anaerobic digestion environments

Bikash Chandra Maharaj[1,2,4], Maria Rosaria Mattei[2], Luigi Frunzo[2], Artin Hatzikioseyian[3], Eric D. van Hullebusch[4,5], Piet N. L. Lens[4] and Giovanni Esposito[6]*

[1]University of Cassino and the Southern Lazio, Department of Civil and Mechanical Engineering, Cassino, Italy
[2]University of Naples Federico II, Department of Mathematics and Applications 'Renato Caccioppoli', Naples, Italy
[3]Laboratory of Environmental Science and Engineering, School of Mining and Metallurgical Engineering, National Technical University of Athens (NTUA), 9 Heroon Polytechniou, 15780, Athens, Greece
[4]IHE Delft Institute for Water Education, Department of Environmental Engineering and Water Technology, The Netherlands
[5]Institut de Physique du Globe de Paris, Sorbonne Paris Cité, Université Paris Diderot, UMR 7154, CNRS, F-75005 Paris, France
[6]University of Naples Federico II, Department of Civil, Architectural and Environmental Engineering, Naples, Italy
**Corresponding author: Department of Civil and Mechanical Engineering, University of Cassino and Southern Lazio, Via di Basio 43, 03043 Cassino, Italy*

ABSTRACT

Trace elements (TEs) are essential for microbial activity in anaerobic environments. They are often added to improve the biogas production rate and yield. Dosing of TEs in anaerobic digestion (AD) systems is largely based on trial-and-error approach as

doi: 9781789060225_0101

no general guidelines exist to date. This is primarily because the fate of TEs in AD environments still remains poorly understood. This knowledge gap is due to the multiple and complex biogeochemical processes influencing TEs chemistry, TE physicochemical interactions with biotic and abiotic surfaces, as well as uptake by microbial community. A mathematical model based on TE-dosing optimization can be recruited to tackle such a complex problem. In this regard, the major physicochemical processes involved in determining the fate of TEs in an anaerobic-digestion environment need to be reviewed and consolidated with a suitable modelling approach. This chapter enlists and describes the most important physicochemical processes such as precipitation, adsorption, and aqueous complexation, as well as the bio-uptake mechanisms involving TEs in AD systems with the aim of summarizing the main modelling contributions to determine the fate of TEs in engineered anaerobic-digestion environments.

KEYWORDS: modeling, anaerobic digestion, trace elements

5.1 INTRODUCTION

Nutrients are essential for living organisms to carry out catabolic and anabolic biochemical reactions. The microbial requirement in terms of nutrients has been manipulated in all bioprocess technologies (England, 2013). Nutrients can be classified in two broad categories: macro- and micro- nutrients. Macronutrients are the bulk of the energy molecules required by the microbes, while micronutrients support the metabolism in the form of structural molecules. Micronutrients also enhance the rate and specificity of biochemical reactions. Accordingly, balanced macro- and micronutrients are required for ideal growth conditions and are essential for efficient and stable biogas production (Fermoso *et al.*, 2008). Any imbalance in these factors can affect the activity and syntrophy of microorganisms in an anaerobic digester (Gustavsson, 2012; Jiang, 2006) and hence limit biogas production. The presence of oxygen, the accumulation of volatile fatty acids (VFAs) and the presence of toxic compounds/elements (i.e. ammonium, high concentrations of TEs) are the major disturbances reported for AD systems (Chen *et al.*, 2008). Among all the microbial communities prevailing in an anaerobic environment, methanogens are the most sensitive to environmental perturbations and hence their activity is easily disturbed.

Table 5.1 lists the most important micronutrients or trace elements (TEs) involved in AD systems and the stimulating concentration range reported in some experimental studies performed with pure microbial strains (Glass & Orphan, 2012). In this regard, Fe, Co an Ni have been recognized as essential micronutrients (Glass & Orphan, 2012; Oleszkiewicz & Sharma, 1990; Thanh *et al.*, 2015; Uemura, 2010). The effect of TEs on AD has been extensively reported (Fermoso *et al.*, 2008; Gonzalez-Gil & Kleerebezem, 1999; Jiang, 2006; Mudhoo & Kumar, 2013; Roussel, 2012; Thanh *et al.*, 2015; Zandvoort *et al.*,

2006). Cobalt forms the core of the vitamin B12 which acts as a cofactor for the enzyme methylase involved in methane production (Banerjee & Ragsdale, 2003; Stupperich & Kräutler, 1988; Mazumder *et al.*, 1987). The coenzyme F430 containing Ni is essential for the functioning of the methylcoenzyme M reductase, which is involved in the reduction of coenzyme M to methane in methanogens (Finazzo *et al.*, 2003; Thauer, 1998). Iron is involved in the transport system of the methanogenic archaea for the conversion of CO_2 to CH_4, where it functions both as an electron acceptor and donor (Thanh *et al.*, 2015), and also binds to sulfide to form precipitates which in turn reduce the hydrogen sulfide content of the anaerobic digester (Gustavsson, 2012; Hille *et al.*, 2004; Kong *et al.*, 2016; Oude Elferink *et al.*, 1994; Shakeri *et al.*, 2012). Similarly, Mn acts as an electron acceptor in anaerobic processes. Zn, Cu, and Ni have all been found in hydrogenase (Thanh *et al.*, 2015). Trace elements such as W and Mo are also found in enzymes such as formate dehydrogenase involved in formate formation from propionate by propionate oxidizers (Thanh *et al.*, 2015). Tungsten can also be considered as essential, but its low concentration in the sludge in comparison with the other metals (Fe, Ni and Co) reduces the interest for supplementing this metal (Fermoso *et al.*, 2009; Oleszkiewicz & Sharma, 1990).

Table 5.1 List of TEs with optimal dissolved concentration in growth media for pure methanogenic cultures grown on different substrates (adapted from Glass & Orphan, 2012).

Metal	Substrate	Concentration (μM)	Species
Fe	H_2/CO_2	300–500	*Methanospirillum hungatei*
	H_2/CO_2	>15	*Methanococcus voltae*
	Acetate	100	*Methanothrix soeggenii*
	Methanol	50	*Methanosarcina bakeri*
Ni	H_2/CO_2	1	*Methanobacterium thermoautotrophicum*
	H_2/CO_2	0.2	*Methanococcus voltae*
	Acetate	2	*Methanothrix soehngenii*
	Methanol	0.1	*Methanosarcina barkeri*
Co	Acetate	2	*Methanothrix soehngenii*
	Methanol	1	*Methanosarcina barkeri*
Mo	Acetate	2	*Methanothrix soehngenii*
	Methanol	0.5	*Methanosarcina barkeri*
W	H_2/CO_2	1	*Methanocorpusculum parvum*
	Formate	0.5	*Methanocorpusculum parvum*

Within biological systems, the physicochemical processes are those that are not directly mediated by microbial activity, but affect the biochemical processes to a

large extent (Batstone *et al.*, 2012). Physicochemical processes including precipitation, co-precipitation, adsorption, surface complexation and gas production are among the most important taking place in AD. These processes occur in the extracellular environment and affect the overall performance of the system by mediating a change in the proton balance (hence in pH) of the bioreactor (Fermoso *et al.*, 2015). In particular, the physicochemical processes are directly related to the fate of TEs in AD and, therefore, to the bioavailability of TEs for bio-uptake. Some of the main physicochemical mechanisms related to TEs in AD are presented in Figure 5.1.

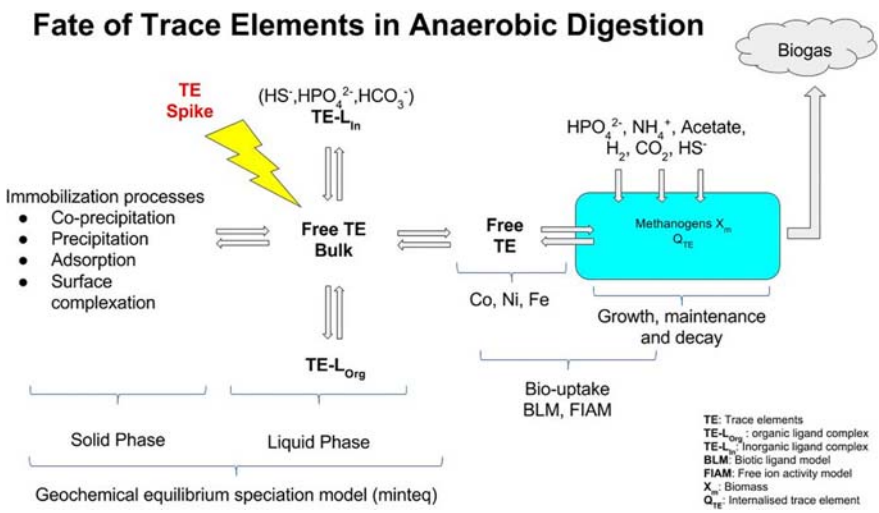

Figure 5.1 Schematic representation of various processes affecting the dynamics of TEs in an engineered anaerobic system.

The underlying principles of the physicochemical processes are relatively well understood (Batstone *et al.*, 2012; Stumm & Morgan, 1996). However, existing AD models, including the Anaerobic Digestion Model 1 (ADM1) as the most representative (Batstone *et al.*, 2002), lack a thoughtful implementation of many of those processes occurring in AD (Batstone *et al.*, 2012; Fermoso *et al.*, 2015; Flores-Alsina *et al.*, 2016; Maharaj *et al.*, 2018; Mbamba *et al.*, 2015a, b; Xu *et al.*, 2015; Zhang *et al.*, 2015).

The understanding and efforts to model and quantify the fate of TEs in AD are isolated and patchy. This chapter attempts to consolidate the available knowledge and efforts on modelling the fate of TEs in AD and envisages a set of processes necessary to quantify the TE dynamics. The chapter presents the principles and methodologies to incorporate the effect of TEs in the structure of AD models. Figure 5.2 summarizes a conceptual interaction diagram between

methane-producing microbes, sulfate-reducing bacteria and TEs. It is clearly depicted that the effect of TEs should be studied in an integrated competing biotic and abiotic environment in an AD model. For all the processes to be discussed in the following sections, the relative models have been classified in two broad categories: the first corresponds to the mathematical models that have been formulated for the specific process independently from the consideration of an AD environment, while the second contemplates the models that can be considered to be an extension of the original ADM1 model. This option is justified by the significant impact that the ADM1 model has on AD literature. Indeed, in the timeline of the published models, ADM1 is considered a significant milestone (Batstone *et al.*, 2002). ADM1 was the result of a collaborative work from the International Water Association (IWA) task group for mathematical modelling of AD processes. The authors tried to unify and consolidate the knowledge and modelling experience accumulated in the literature until 2002, when the scientific and technical report of ADM1 was first published (Batstone *et al.*, 2002). ADM1 is considered even today a state-of-the-art model, including a significant number of biological, chemical and physicochemical processes (Batstone *et al.*, 2002). The model was conceived as a general modelling framework for AD processes and as such has been used successfully without modifications (Blumensaat & Keller, 2005) or in a modified version (Galí *et al.*, 2009; Parker & Wu, 2006; Peiris *et al.*, 2006) by many researchers to simulate experimental results. ADM1 has also been used as a complementary module to activated sludge models such as activated sludge model 1 (ASM1), activated sludge model 2d (ASM2d) or activated sludge model 3 (ASM3) for plant-wide wastewater treatment processes (Copp *et al.*, 2003; Kauder *et al.*, 2007; Lopez-Vazquez *et al.*, 2013; Nopens *et al.*, 2009; Rosen *et al.*, 2006).

Note that the majority of mathematical models under consideration in this work do not explicitly consider TEs as model components. However, such models are discussed as they introduce a general framework that could be extended/adapted to the case of TEs in AD systems. Furthermore, as the mathematical modelling of the fate of TEs in AD systems cannot neglect the explicit consideration of sulfur and phosphorus dynamics, which play a crucial role in precipitation and adsorption processes, the main mathematical models accounting for sulfur and phosphorus in anaerobic environments have been reviewed as well.

This chapter is organized as follows: in Section 5.2 the main models for sulfur and phosphorus dynamics in anaerobic environments are described. In Section 5.3 the main physicochemical processes affecting TE availability in AD systems are described and the modelling approaches proposed over the years are reviewed and summarized. Specifically, Section 5.3.1 is dedicated to precipitation modelling; in Section 5.3.2 adsorption mechanisms and the main modelling approaches to this topic are presented; Section 5.3.3 is devoted to aqueous complexation and the relative modelling approaches. The chapter has been extended with Section 5.4

which refers to the mathematical modelling of TEs bio-uptake and reviews the mathematical formulas usually adopted for dose-response functions.

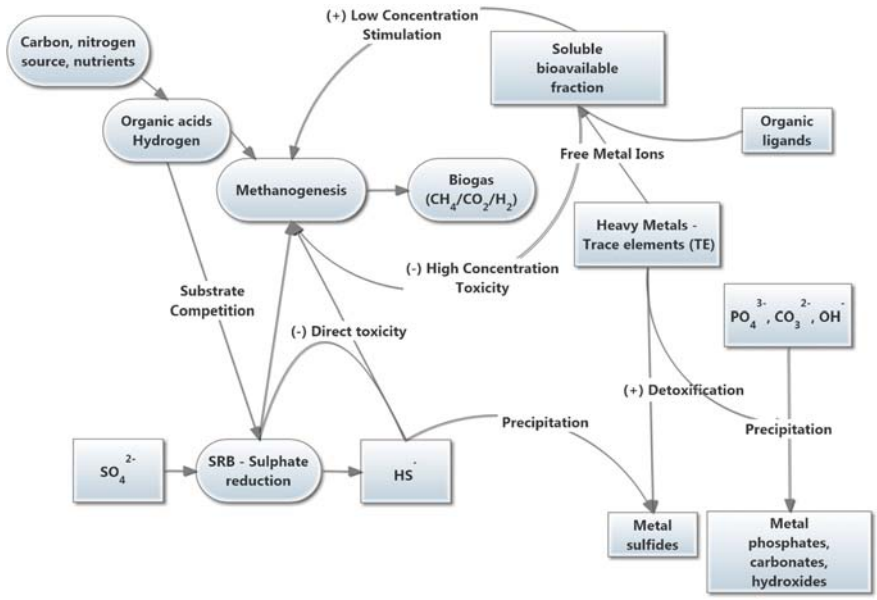

Figure 5.2 Conceptual interactions between methanogenic activity, sulfate reduction and trace elements positive (+) or negative (−) effects on biogas production.

5.2 MATHEMATICAL MODELLING OF SULFUR AND PHOSPHORUS CYCLES IN ANAEROBIC DIGESTION SYSTEMS

5.2.1 Sulfur modelling

Sulfur represents a dominant element in anaerobic digesters, counting on multiple sources. In particular, sulfide precipitates have been identified as one of the major sinks for sulfur-related compounds and subsequent removal of heavy metals toxicity (Lawrence & McCarty, 1965). Due to the significant participation of sulfur compounds in physicochemical processes affecting TEs fate and bioavailability in AD systems, it is necessary to consider sulfur transformations such as sulfate reduction in AD models (Paulo *et al.*, 2015). In this regard, ADM1 lacks the representation of sulfur bioprocesses. The extension of any AD models with sulfate-reduction processes is considered prerequisite when TEs are also included in the system. This is related to the fact that most TEs form stable insoluble solid sulfide precipitates under sulfidogenic conditions. This process

significantly affects the bioavailable fraction of TEs and cannot be ignored (Paulo *et al.*, 2015). Nonetheless, some studies have been carried out for modelling sulfate reduction in AD. Sulfate-reduction modelling necessitates the definition of important biochemical, gas transfer, and physicochemical process rates to link new state variables. These processes and state variables are mentioned along with the modelling efforts discussed in the following sections.

Sulfate-reduction models have been developed and calibrated for specific purposes for different substrates and for simulating specific systems. Some follow a different principle (other than ADM1) in their conception and hence they are classified in this chapter as 'stand-alone sulfate-reduction models' (Kalyuzhnyi & Fedorovich, 1997, 1998; Knobel & Lewis, 2002; Poinapen & Ekama, 2010; Ristow *et al.*, 2002; Vavilin *et al.*, 1995). Conversely, models which are embedded in the structure of ADM1 have been termed as 'ADM1-based sulfate-reduction models' (Barrera *et al.*, 2015; Federovich *et al.*, 2003; Flores-Alsina *et al.*, 2016). These two groups of models are discussed in the following sections.

5.2.1.1 Stand-alone sulfate-reduction models

Sulfate-reduction models have evolved independently as well as part of more complex AD models. These models do not follow the ADM1 structure as the theoretical basis, for some of them were already set before the inception of ADM1. In an attempt to model the physicochemical reaction system for pH prediction, a simulation model for AD was developed (Vavilin *et al.*, 1995). The model kept track of the sulfide formation and its effect on pH. It also considered two sulfate-reducing microbial groups which separately use acetate and propionate as organic substrate to produce sulfide from sulfate. A reduced model of self-oscillating dynamics in an AD system with sulfate reduction was developed in (Kalyuzhnyi & Fedorovich, 1998). The model considered only two groups of microbes, methanogens and sulfate reducers. Substrate-limiting functions were described by typical Monod equations. The model considered hydrogen sulfide inhibition as a function of non-ionized hydrogen sulfide. Finally, the model was validated with experimental data. The competition between sulfate-reducing bacteria (SRB) and methanogens by using data from a synthetic high sulfate-containing wastewater treated in a UASB reactor was evaluated in (Kalyuzhnyi & Fedorovich, 1998). There was a good correlation between model simulations and experimental data. Competition for acetate was emphasized. The modelling results were obtained under variations of hydraulic retention time (HRT), SO_4^{2-}/COD ratio, initial proportion of SRB/methanogens in seed sludge, efficiency of retention of SRB, and sludge retention time. Similarly, the competition between methanogens and SRB in a UASB reactor was studied to develop a dispersed plug-flow model (Kalyuzhnyi *et al.*, 1998). Data from literature were used to calibrate the model with emphasis on acetate competition. The model was able to predict system performance with regard to

variations in the liquid upward velocity as an important control parameter. However, when pH changes occurred the results were not correctly predicted. The model of Knobel and Lewis (2002) was calibrated and validated for a number of reactor configurations: packed bed, UASB and gas lift reactor. Three simulation studies were carried out in steady-state and dynamic conditions. The first two simulation tests were able to predict concentration of sulfate and COD in the effluent. AQUASIM was used (Ristow *et al.*, 2002) in a recycling sludge bed reactor to simulate the AD process including sulfate reduction. Acid-mine drainage and primary sludge were used as sulfate-containing wastewater and carbon source, respectively. Data from pilot plant agreed well with model simulations. Influence of sludge recycle ratio, SO_4^{2-}, COD ratio and HRT on sulfate-reduction process was studied. A two-phase (aqueous-gas) kinetic model for sulfate-reduction processes using primary sewage sludge as carbon source was developed in Poinapen & Ekama 2010. The kinetic model was calibrated with experimental data starting from different SO_4^{2-}/COD ratios (Poinapen & Ekama 2010). Model simulations showed better fitting with experimental data. In addition, model simulations showed that at ambient temperature of 20°C, the hydrolysis rate is significantly reduced as compared with 35°C. The hydrolysis rate of the primary sewage sludge biodegradable particulate organism is the same under methanogenic and sulfidogenic conditions. The primary sewage sludge and biodegradable particulate organics are carbon deficient for biological sulfur reduction. Moreover, the model only considered gas stripping for H_2S. The efficiency of retention of SRB, HRT, SO_4^{2-}, butyrate, propionate, and acetate were predicted. However, the removal efficiencies for COD, SO_4^{2-}, hydrogen sulfide concentrations in the gas phase were not predicted (Barrera *et al.*, 2013). In summary, 'stand-alone sulfur-reduction models' have been developed and calibrated to study the impact of operating parameters and initial concentrations under specific cases.

5.2.1.2 ADM1-based sulfate-reduction models

Sulfate-reduction processes as an extension of ADM1 have been implemented in Federovich *et al.* (2003). The model was calibrated against experimental data from literature and was able to predict sulfate removal in the AD process, the concentrations of butyrate, propionate and acetate, as well as methane and biomass production. The extended model included sulfate reduction and biogenic sulfide production by SRB. SRB compete with methanogens for intermediates produced during the biodegradation processes. The extension added four different SRB species ($X_{\text{SRB butyrate}}$, $X_{\text{SRB propionate}}$, $X_{\text{SRB acetate}}$, $X_{\text{SRB hydrogen}}$) which oxidize butyrate, propionate, acetate and hydrogen, respectively, coupled with sulfate reduction according to the following reactions:

$$2C_3H_7COO^- + SO_4^{2-} \xrightarrow{X_{\text{SRB butyrate}}} 4CH_3COO^- + H^+ + HS^- \quad (5.1)$$

$$4C_2H_5COO^- + 3SO_4^{2-} \xrightarrow{X_{\text{SRB propionate}}} 4CH_3COO^- + 4HCO_3^- + H^+ + 3HS^- \quad (5.2)$$

$$CH_3COO^- + SO_4^{2-} \xrightarrow{X_{\text{SRB acetate}}} 2HCO_3^- + HS^- \quad (5.3)$$

$$4H_2 + H^+ + SO_4^{2-} \xrightarrow{X_{\text{SRB hydrogen}}} HS^- + 4H_2O \quad (5.4)$$

The following rate equations for reactions (5.1)–(5.4) have been adopted:

$$r_i = k_{\max,i} \frac{S_i}{K_{S_i} + S_i} \cdot \frac{S_{SO_4}}{K_{SO_4} + S_{SO_4}} \cdot X_i \cdot I_{\text{pH}} \cdot I_{\text{sulfide}} \quad (5.5)$$

where r_i is the volumetric growth rate of SRB group X_i [M L^{-3} T^{-1}], $k_{\max,i}$ is the maximum specific growth rate for group X_i [T^{-1}], S_i represents the concentration of substrate i [M L^{-3}], K_{Si} denotes the Monod half-saturation constant for substrate i [M L^{-3}], S_{SO_4} is the concentration of sulfate in liquid phase [M L^{-3}], K_{SO4} represents the Monod half-saturation constant for sulfate [M L^{-3}], X_i is the concentration of SRB biomass group i [M L^{-3}], I_{pH} is the pH inhibition factor (dimensionless), and I_{sulfide} represents the sulfide inhibition factor (dimensionless). The inhibition by hydrogen sulfide was included in the rate equation (5.5) through the term:

$$I_{\text{sulfide}} = 1 - \frac{S_{H_2S}}{K_I} (if\ S_{H_2S} > K_I, I_{\text{sulfide}} = 0) \quad (5.6)$$

where S_{H_2S} denotes the concentration of undissociated hydrogen sulfide in liquid phase [M L^{-3}]; and K_I is the inhibition constant of undissociated hydrogen sulfide [M L^{-3}].

The values of the kinetic parameters for SRB were estimated in the model to simulate the behavior of a UASB fed with sulfate up to 6 g S/L (Federovich *et al.*, 2003). Although this model is reported today as the most appropriate extension of ADM1 when sulfate-removal efficiencies are of primary interest, it was not calibrated to predict the concentrations of total aqueous sulfide, undissociated sulfides and gas phase sulfides.

Similarly, an extension of ADM1 with sulfate reduction was proposed in (Barrera *et al.*, 2015). The model was calibrated and validated for a high strength and sulfate rich wastewater (cane molasses vinasse). Butyric acid was neglected as substrate for SRB in the model structure. Propionic acid, acetic acid, hydrogen were considered as primary electron donors for sulfate reduction processes. Propionate SRB, acetate SRB and hydrogenotrophic SRB were considered in addition to the seven microbial groups of ADM1. The new biochemical reactions introduced in the model have been depicted in the following equations:

$$C_2H_5COOH + 0.75H_2SO_4 \xrightarrow{X_{\text{SRB propionate}}} CH_3COOH + CO_2 + H_2O + 0.75H_2S \quad (5.7)$$

$$CH_3COOH + H_2SO_4 \xrightarrow{X_{\text{SRB acetate}}} 2CO_2 + 2H_2O + H_2S \tag{5.8}$$

$$4H_2 + H_2SO_4 \xrightarrow{X_{\text{SRB hydrogen}}} H_2S + 4H_2O \tag{5.9}$$

A dual Monod type kinetic was used for the uptake of the substrates. Protonation and deprotonation of sulfuric acid and sulfide ions were considered in the liquid phase. Gas stripping of H_2S was also considered. S_{H_2S} was included as the process inhibitor. Likewise, a non-competitive inhibition function for sulfides was introduced. The model prediction works reasonably well for the process variables with an accurate quantitative predictions of high ($\pm 10\%$) to medium (10%–30%) and error ranging from 1 to 26%.

Recently in (Flores-Alsina *et al.*, 2016), biological production of sulfide by sulfate reducing bacteria has been included as one of the four extensions to ADM1, the others being phosphorus metabolism, mineral precipitation and iron transformation in an AD system. The model was applied to a set of full-scale plant-wide data.

Selected process rates and inhibition functions, which may be used to model sulfate reduction processes, are represented in the equations below. Readers may refer to the literature for more details (Barrera *et al.*, 2013).

Growth rate for SRB species:

$$r_i = k_{\max,i} \frac{S_i}{K_{S_i} + S_i} \cdot \frac{S_{SO_4}}{K_{SO_4} + S_{SO_4}} \cdot X_i \cdot I_{pH} \cdot I_{H_2S} \tag{5.10}$$

where, r_i is the volumetric growth rate of SRB group $i[ML^{-3}T^{-1}]$; $k_{\max,i}$ is the maximum specific growth rate of SRB group $i[T^{-1}]$; S_i is the concentration of soluble organic components $[ML^{-3}]$; K_{S_i} is half saturation constant $[ML^{-3}]$; X_i is the concentration of SRB group $i[ML^{-3}]$; I_{pH} is the pH inhibition function; and I_{H_2S} is the sulfide inhibition function.

Biomass decay rate:

$$r_{\text{decay},i} = k_{\text{dec},i} \cdot X_i \tag{5.11}$$

where, $\rho_{\text{decay},i}$ is the kinetic rate of substrate uptake (kg COD $m^3 d_{-1}$); and $k_{\text{dec},i}$ is first order decay rate of species $i(d^{-1})$;

Acid-base rate for sulfide species:

$$\rho_{A/B} = K_{A/B,H_2S}(S_{HS^-} \cdot (S_{H^+} + K_{a,H_2S}) - K_{a,H_2S} \cdot S_{H_2S,\text{tot}}) \tag{5.12}$$

where $\rho_{A/B}$ is the acid-base kinetic rate $[ML^{-3}T^{-1}]$; $k_{A/B,H_2S}$ is the acid-base kinetic parameter $[M^{-1}L^3T^{-1}]$; S_{HS^-} is the concentration of bisulfide ion $[ML^{-3}]$; S_{H^+} is the concentration of hydrogen ion $[ML^{-3}]$; $S_{H_2S,\text{tot}}$ is the concentration of total H_2S species (dissociated and undissociated) in liquid phase $[ML^{-3}]$; and K_{a,H_2S} is the acid-base equilibrium coefficient $[ML^{-3}]$.

Gas transfer:

$$\rho_{gas} = k_l a \cdot (S_{H_2S} - K_{H,H_2S} \cdot P_{gas,H_2S}) \tag{5.13}$$

where ρ_{gas} is the specific mass transfer rate of gas $H_2S[ML^{-3}T^{-1}]$; $k_l a$ is the gas-liquid mass transfer coefficient $[T^{-1}]$; S_{H_2S} is the concentration of undissociated $H_2S[ML^{-3}]$ K_{H,H_2S} is Henry's law coefficient $[M^2L^{-3}T^{-1}]$; and P_{gas,H_2S} is the partial pressure of the H_2S gas$[MT^{-1}]$.

Process inhibition:

Sulfide:

$$I_{H_2S} = e^{-\left(\frac{S_{H_2S}}{K_{I,H_2S}}\right)^2} \tag{5.14}$$

where K_{I,H_2S} is the inhibition coefficient by undissociated $H_2S[ML^{-3}]$.

$$I_{H_2S} = \frac{1}{1 + \dfrac{S_{H_2S}}{K_{I,H_2S}}} \tag{5.15}$$

$$I_{H_2S} = \frac{1}{1 + \left(\dfrac{S_{H_2S}}{K_2}\right)^{\ln 99/\left(\frac{K_{100}}{K_2}\right)}} \tag{5.16}$$

where K_{100} is the concentration of H_2S or pH at which the uptake rate is decreased 100 times $[ML^{-3}]$; and K_2 is the concentration of H_2S or pH at which the uptake rate is decreased 2 times $[ML^{-3}]$.

pH:

$$I_{pH} = \frac{1}{1 + \dfrac{pH^{\ln 99/(K_{100}/K_2)}}{K_2}} \tag{5.17}$$

where pH is the resultant or predicted pH of the system.

$$I_{pH} = (1 + \exp(-\alpha_{LL}(pH - pH_{LL})))^{-1} \cdot (1 + \exp(-\alpha_{UL}(pH - pH_{UL})))^{-1} \tag{5.18}$$

where α_{LL} and α_{UL} are the parameters which affect the steepness of the curve; pH_{LL} is the lower pH limit where microbial growth is 50% inhibited; and pH_{UL} is the upper pH limit where microbial growth is 50% inhibited.

$$I_{pH} = \frac{1 + 2 \cdot 10^{0.5(pH_{UL} - pH_{LL})}}{1 + 10^{(pH - pH_{UL})} + 10^{(pH_{LL} - pH)}} \tag{5.19}$$

5.2.2 Phosphorus modelling

Phosphorus is one of the most abundant inorganic components of AD systems (~30% nutrient load according to Johnson and Shang (2006)). Phosphorus transformations are major drivers for precipitation processes (struvite precipitation). Although phosphorus precipitation has been addressed in equilibrium- and kinetic-based models, phosphorus transformations have not been linked to the biodegradation reactions in the majority of studies. Poly-hydroxy-alkanoates (X_{PHA}), poly-phosphate (X_{PP}), and phosphate ($S_{PO_4^{3-}}$) are the major biochemical components which are necessary to define phosphorus transformations. Apart from this, inorganic phosphate-water acid/base system ($S_{PO_4^{3-}}/S_{HPO_4^{2-}}/S_{H_2PO_4^-}/S_{H_3PO_4}$) should be taken into account to track the change in pH. Additionally, based on requirements, inorganic phosphate minerals can also be introduced, such as, amorphous calcium phosphate ($X_{Ca_3(PO_4)_2}$), hydroxylapatite ($X_{Ca_5(PO_4)_3(OH)}$), octacalium phosphate ($X_{Ca_8H_2(PO_4)_6}$) and, struvite ($X_{MgNH_4PO_4}$). The following lines briefly discuss efforts to model phosphorus transformations in waste-treatment models and ADM1-based models.

Modelling the effect of pH change (due to phosphate species) and tracking the dynamics of phosphate minerals in relation to the biodegradation are two important aspects of modelling phosphorus in AD systems. The pH prediction module has been expanded to take into account physicochemical effects such as ion-activity correction, ion-pairing behavior, and weak acid-base reactions occurring in conjugation with biological reactions (Solon *et al.*, 2015). Phosphorus metabolism has been implemented in the framework of ADM1 in (Johnson & Shang, 2006). Two major methods for incorporating phosphorus in the AD models have been identified (Solon, 2015). In the first approach, P does not participate in biological reactions. The quantity of phosphorus within the system, i.e. in the particulate and soluble components, is tracked through the introduction of a new state variable S_{IP} (concentration of inorganic phosphorus). This acts as the only source and sink for all the inorganic phosphorous minerals and acid-base species (Zaher & Chen, 2006; Zaher *et al.*, 2007). In addition, it is assumed that there are instantaneous phosphorus-related processes taking place at the interface between the activated sludge and the AD process. The prevalence of inorganic phosphorus and absence of biological phosphorus oversimplifies the model structure.

Conversely, the alternate method takes into account some of the processes which are considered in the IWA Activated Sludge Model No. 2d (ASM2d) (Henze *et al.*, 1999). These processes are further incorporated in ADM1. Phosphorus metabolizing microorganisms are active in the anaerobic digester and facilitate microbial conversion of phosphate-related compounds. Based on this principle, a model was developed in (Wang *et al.*, 2016). The model investigated anaerobic fermentation of enhanced biological phosphorus removal of sludge in terms of phosphate release and VFA production with respect to

polyphosphate-accumulating organism (PAO) activity. The proposed model extension included: (a) the storage of 4 VFA as PHA mediated by PAOs; (b) the effect of PHA content on disintegration rate; and (c) the mineral phosphate precipitation. Similar to this study, a new extension was implemented which enabled the release of phosphorus in AD (Flores-Alsina *et al.*, 2016). For this, phosphorus-accumulating organism (X_{PAO}), polyhydroxyalkanoates (X_{PHA}) and polyphosphates (X_{PP}) constitute the new state variables. Seven new processes were added for: (a) uptake of valerate, butyrate, propionate and acetate to form polyhydroxyalkanoates (X_{PHA}); (b) decay of phosphorus accumulating organism (X_{PAO}); and (c) lysis of polyhydroxyalkanoates (X_{PHA}) and polyphosphates (X_{PP}). Further details of the model can be found in the literature (Flores-Alsina *et al.*, 2016).

5.3 MATHEMATICAL MODELLING OF PHYSICOCHEMICAL PROCESSES IN ANAEROBIC DIGESTION SYSTEMS

Despite several efforts devoted to the improvement of physicochemical modelling and simulation in anaerobic environments, the effect and fate of TEs have not been accounted for (Fermoso *et al.*, 2015; Lauwers *et al.*, 2013; van Hullebusch *et al.*, 2016). As mentioned, the most important processes to be included in the AD model in order to estimate the fate of TEs are: precipitation, aqueous complexation and surface complexation/adsorption (Batstone *et al.*, 2012; van Hullebusch *et al.*, 2016). A modelling approach is envisioned that takes into account all these intermittent processes and unifies them in the form of a defined model structure (Figure 5.2 above). In the last decades, there have been efforts in wastewater-treatment process modelling to predict the physico-chemical state of the system. A list of such efforts has been provided in Table 5.2. Some of these works are discussed in the following lines. In addition, the ADM1 extensions considering the mentioned processes are also described.

5.3.1 Precipitation

With the term 'non ADM1-based precipitation models', we refer to the class of models that have been developed to simulate the precipitation process in aqueous environments, non-necessarily anaerobic. In some cases such models account for the biodegradation reactions occurring in AD but they do not follow the modelling framework introduced in ADM1. Conversely, we define 'ADM1-based precipitation models', the ones that have been conceived in the framework of ADM1 and explicitly take into account precipitation reactions not necessarily for TEs. Table 5.3 represents a potential list of precipitation reactions which can occur in an anaerobic environment.

Table 5.2 Waste-treatment models considering various processes involving geochemical components.

No.	Reference	Process	Model Type	Geochemical Components	Application	
1	Hanhoun *et al.* (2011)	Precipitation	Equilibrium	Mg^{2+}, NH_4^+, PO_4^{3-}, H_2O	Phosphorus recovery	Lab scale
2	Scott *et al.* (1991)	Precipitation	Equilibrium	Mg^{2+}, NH_4^+, PO_4^{3-}, H_2O	Waste water stream, kidney stones	Lab scale
3	Barat *et al.* (2011)	Precipitation	Equilibrium, Kinetic	Mg^{2+}, NH_4^+, PO_4^{3-}, H_2O, CO_3^{2-}, Ca^{2+}, K^+	SBR for biological phosphorus removal	Lab scale
4	Musvoto *et al.* (2000b)	Acid-base reactions, precipitation, gas stripping, ion pairing	Kinetic	H^+, OH^-, H_2CO_3, HCO_3^-, CO_3^{2-}, H_3PO_4, $H_2PO_4^-$, HPO_4^{2-}, PO_4^{3-}, NH_4^+, Ca^{2+}, Mg^{2+}	Aeration of anaerobic digestion liquor from spent wine UASB and AD for sewage sludge	Plant wide
5	Maurer & Boller (1999)	Precipitation	Kinetic	H_2CO_3, HCO_3^-, CO_3^{2-}, OH^-, H^+, H_3PO_4, $H_2PO_4^-$, HPO_4^{2-}, PO_4^{3-}, Ca^{2+}	Waste treatment-EBPR	Lab scale
6	Ohlinger *et al.* (1998)	Precipitation	Equilibrium	Mg^{2+}, PO_4^{3-}, HPO_4^{2-}, OH^-, H^+, NH_4^+	Waste treatment	Plant wide
7	Smith *et al.* (2008)	Precipitation, adsorption, co-precipitation	Equilibrium	H^+, PO_4^{3-}, Fe^{2+}	Phosphate removal	Lab scale
8	Wrigley *et al.* (1992)	Precipitation	Equilibrium	Mg^{2+}, NH_4^+, PO_4^{3-}, H_2O	Waste water stream, kidney stones	Lab scale
9		Precipitation	Kinetic		Waste treatment	Lab scale

	Van Rensburg *et al.* (2003)			H^+, OH^-, H_2CO_3, HCO_3^-, CO_3^{2-}, H_3PO_4, $H_2PO_4^-$, HPO_4^{2-}, PO_4^{3-}, NH_4^+, Ca^{2+}, Mg^{2+}		
10	Tait *et al.* (2009)	Precipitation	Equilibrium		Low cost sulfate removal	Lab scale
11	Hauduc *et al.* (2015)	Acid-base; chemical ion pairing; precipitation; chemical surface complexation; adsorption; co-precipitation	Kinetic	Multiple components	Chemical phosphorus removal	Lab scale
12	Schwarz & Rittmann (2007)	Acid-base reactions, Precipitation, surface complexation, biodegradation	Equilibrium, Kinetic,	HS^-, S^-, H^+, Zn^{2+}	Metal detoxification in sulfidic systems	Lab Scale
13	Mbamba *et al.* (2015b)	Acid base, precipitation-dissolution, gas stripping	Equilibrium, Kinetic	H^+, NH_4^+, Ca^{2+}, Mg^{2+}, PO_4^{3-}, PO_4^{3-}	Calcite precipitation in synthetic aqueous solution	Lab scale
14	Flynn *et al.* (2014)	Surface complexation	Equilibrium	Co, Ni, Sr, Zn	Calculation of metal-carboxyl bacterial surface stability constant	Lab scale
15	VanBriesen & Rittmann (1999)	Acid-base, complexation and biodegradation	Equilibrium, Kinetic	H^+, NH_4^+, OH^-, Fe^{3+}, H_2CO_3	Citrate/Fe(III) systems	Theoretical

Table 5.3 Probable precipitation reactions in AD systems.

No.	Name	Precipitation Reaction	LogK_{sp}	Citation in AD systems
1	Al_2O_3	$Al_2O_3 + 6H^+ \rightleftharpoons 2Al^{3+} + 3H_2O$	19.6	Mu *et al.* (2011)
2	$AlPO_4$	$AlPO_4 \rightleftharpoons Al^{3+} + PO_4^{3+}$	20.2	Peng & Colosi (2016)
3	Anhydrite	$CaSO_4 \rightleftharpoons Ca^{2+} + SO_4^{2-}$	4.6	MacConnell & Collins (2009)
4	Aragonite	$CaCO_3 \rightleftharpoons Ca^{2+} + CO_3^{2-}$	8.3	Musvoto *et al.* (2000b)
5	Brucite	$Mg(OH)_2 + 2H^+ \rightleftharpoons Mg^{2+} + 2H_2O$	17.1	Uludag-Demirer & Othman (2009)
6	$CaHPO_4$	$CaHPO_4 \rightleftharpoons Ca^{2+} + H^+ + PO_4^{3-}$	19.2	Van Langerak *et al.* (1999)
7	$Ca_4H(PO_4)_3 \cdot 3H_2O$	$Ca_4H(PO_4)_3 \cdot 3H_2O \rightleftharpoons 4Ca^{2+} + H^+ + 3PO_4^{3-} + 3H_2O$	47.9	Zhang *et al.* (2010)
8	Calcite	$CaCO_3 \rightleftharpoons Ca^{2+} + CO_3^{2-}$	8.4	Mbamba *et al.* (2015a,b)
9	$Ca_3(PO_4)_2$	$Ca_3(PO_4)_2 \rightleftharpoons 3Ca^{2+} + 2PO_4^{3-}$	25.5	Ye *et al.* (2010)
10	Dolomite	$CaMg(CO_3)_2 \rightleftharpoons Ca^{2+} + Mg^{2+} + 2CO_3^{2-}$	16.5	Musvoto *et al.* (2000b)
11	$Fe(OH)_2$	$Fe(OH)_2 + 2H^+ \rightleftharpoons Fe^{2+} + 2H_2O$	12.8	Dezham *et al.* (1988)
12	FeS	$FeS + H^+ \rightleftharpoons Fe^{2+} + HS^-$	2.9	Fermoso *et al.* (2015)
13	Gibbsite	$Al(OH)_3 + 3H^+ \rightleftharpoons Al^{3+} + 3H_2O$	7.7	Qiao & Ho (1996)
14	Huntite	$CaMg_3(CO_3)_4 \rightleftharpoons 3Mg^{2+} + Ca^{2+} + 4CO_3^{2-}$	29.9	Musvoto *et al.* (2000a)
15	Hydroxyapatite	$Ca_{10}(PO_4)_6(OH)_5 + 5H^+ \rightleftharpoons 10Ca^{2+} + 6PO_4^{3-} + 5H_2O$	44.3	Maurer *et al.* (1999)
16	Mackinawite	$FeS + H^+ \rightleftharpoons Fe^{2+} + HS^-$	3.6	Morse & Arakaki (1993)
17	Magnesite	$MgCO_3 \rightleftharpoons Mg^{2+} + CO_3^{2-}$	7.4	Van Rensburg *et al.* (2003)
18	$Mg(OH)_2$	$Mg(OH)_2 + 2H^+ \rightleftharpoons Mg^{2+} + 2H_2O$	18.7	Huang *et al.* (2016)
19	$Mg_3(PO_4)_2$	$Mg_3(PO_4)_2 \rightleftharpoons 3Mg^{2+} + 2PO_4^{3-}$	23.2	Musvoto *et al.* (2000a)
20	Newberyite	$MgHPO_4 \cdot 3H_2O \rightleftharpoons Mg^{2+} + H^+ + PO_4^{3-} + 3H_2O$	18.1	Musvoto *et al.* (2000a)
21	Portlandite	$Ca(OH)_2 + 2H^+ \rightleftharpoons Ca^{2+} 2H_2O$	22.7	Gu *et al.* (2015)
22	Siderite	$FeCO_3 \rightleftharpoons Fe^{2+} + CO_3^{2-}$	10.5	Preis & Gamsjäger (2001)
23	Struvite	$MgNH_4PO_4 \cdot 6H_2O \rightleftharpoons Mg^{2+} + NH_4^+ + PO_4^{3-}$	13.2	Musvoto *et al.* (2000a)
24	Vaterite	$CaCO_3 \rightleftharpoons Ca^{2+} + CO_3^{2-}$	7.9	Musvoto *et al.* (2000a)
25	Vivianite	$Fe_3(PO_4)_2 \cdot 8H_2O \rightleftharpoons 3Fe^{2+} + 2PO_4^{3-} + 8H_2O$	37.7	Roussel & Carliell-Marquet (2016)

5.3.1.1 Non-ADM1-based precipitation models

Precipitation reactions in wastewater systems have been extensively studied in the last few decades (Barat *et al.*, 2011; Donoso-Bravo *et al.*, 2013; Hanhoun *et al.*, 2011; Mbamba *et al.*, 2015a, b; Maurer *et al.*, 1999; Musvoto *et al.*, 2000a, b; Rittmann *et al.*, 2002; Tait *et al.*, 2009; Van Rensburg *et al.*, 2003). Generally, the precipitation studies focus on nutrient removal or recovery from wastewater streams. Recovery of phosphate is central to these studies. This is largely due to the associated risk of water eutrophication (Hauduc *et al.*, 2015; Jimenez *et al.*, 2015; Rahaman *et al.*, 2014; Smith *et al.*, 2008; Szabó *et al.*, 2008). Some of these studies have been supplemented with process models. Different modelling techniques have been used to estimate the precipitation process and the effect of precipitation on the biochemical system (Mbamba *et al.*, 2015b). In general, these modelling strategies are restricted either to thermodynamic equilibrium calculations or to a kinetic approach, and only a minor number of these studies adopted a combination of equilibrium and kinetic approaches to estimate the exent of precipitation (Barat *et al.*, 2011). These approaches and the relative contributions have been listed in Table 5.4 and are discussed below.

The thermodynamic equilibrium method for estimating precipitation makes use of a well established multicomponent thermodynamic equilibrium approach (Allison *et al.*, 1991; Morel & Morgan, 1972; Rittmann *et al.*, 2002). Thermodynamic models consider a system comprising of components and species. Components can interact to form species, but individual species do not react to form new species. This modelling approach assumes the acid-base system to consist of a predefined number of organic/inorganic components and species. All acid-base reactions in the system are considered to be in equilibrium. The system of equation is solved by the Newton-Raphson algorithm using the equilibrium constants and the law of mass action (Mbamba *et al.*, 2015b; Solon *et al.*, 2015). A thermodynamic model for phosphate precipitation was developed to study the effect of pH, ionic strength and temperature on struvite solubility (Hanhoun *et al.*, 2011). In the first step, experiments were conducted to determine the solubility product of struvite from synthetic solution at various temperatures. In the second step, an algorithm was developed to calculate the equilibrium constants. The algorithm is based on a hybrid resolution procedure which integrates a multi-genetic algorithm and the Newton-Raphson method in order to increase computing efficiency. Using this approach, the precipitation of struvite was predicted both quantitatively and qualitatively.

A predictive approach, to determine the amount of precipitate formed when arbitrary amounts of N, Mg and P were added in wastewater system, was developed by (Scott *et al.*, 1991; Wrigley *et al.*, 1992). The computer program used NH_3 as the central species for calculating the precipitated composition. It also included a routine to calculate the activity coefficients of each species involved. After selecting H^+ and Mg^{2+} as main species, concentration ratios (K)

Table 5.4 Representative kinetic equations for mineral-precipitation modelling.

No.	Reference	Model Equations	Notation
1	Ali & Schneider (2008)	$SI = \log\left(\frac{P_{SO}}{P_{cs}}\right)^{1/v}$ $G = KS^n$ $\frac{dM}{dt} = \frac{1}{2}KN\pi\rho_c L^2 S^n L^n$	where • SI is the saturation index; • P_{SO} is the concentration of total species; • P_{cs} is the conditional solubility product; • v is the number of reactants; • G is the growth rate of crystals; • K is a kinetic parameter; • n is a kinetic parameter; • N is the crystal number; • ρ_c is the density of the crystals; • L is the final size of the crystal; • S is the function of supersaturation of crystal; • M is concentration of precipitated crystal.
2	Ebigbo *et al.* (2012)	$SI = \frac{\gamma_i m_i + \gamma_j m_j}{k_{sp}}$	where • SI is the saturation index; • γ_i and γ_j are the activity coefficient of the components; • k_{sp} is the solubility product; • m_i and m_j are the concentration of the components.
3	Jeen *et al.* (2012)	$R_i^m = K_{eff,i}\left(\frac{IAP_i^m}{k_i^m}\right)^{-1}$	where • R_i^m is the rate of mineral precipitation; • $K_{eff,i}$ is the effective rate constant of precipitation; • IAP_i^m is the activity product; • k_i^m is the equilibrium constant for dissolution.

4	Mbamba *et al.* (2015a,b)	$r_{cryst} = k_{cryst} X_{cryst} \sigma^n$ $\sigma = k_{cryst} X_{cryst} \left(\left(\frac{Z_i Z_j}{k_{sp}} \right)^{1/v} - 1 \right)^n$	where • r_{cryst} is the rate of crystallization; • k_{cryst} is the kinetic rate constant for crystallization; • X_{cryst} is the concentration of crystal formed; • σ is the saturation index; • Z_i and Z_j are the concentrations of participating components; • v is the summation of charges; • n is an experimentally determined constant; • k_{sp} is the solubility product.
5	Rittmann *et al.* (2002)	$R_p = k'_a \left(1 - \frac{k_{sp}}{Q} \right) Me$	where • R_p is the rate of precipitation; • Me is the concentration of cationic species (i.e. TEs); • k'_a is the lumped product of reaction or mass transfer rate times; • a is the specific surface area; • k_{sp} is the solubility product; • Q is the reaction product of precipitate.
6	Koutsoukos *et al.* (1980)	$\frac{d[M_{v+}A_{v-}]}{dt} = k_r \left[[[M^{m+}]^{v+} - [A^{a-}]^{v-}]^{1/v} - (k'_{sp})^{1/v} \right]^n$	where • k_r is a kinetic constant; • $[M^{m+}]$ and $[A^{a-}]$ are the ion concentration; • $[M_{v+}A_{v-}]$ is the mineral precipitate concentration; • k'_{sp} is the solubility product; • v is the summation of opposite charges $v^+ + v^-$; • n is a constant with value 2 for sparingly soluble salts.

(*Continued*)

Table 5.4 Representative kinetic equations for mineral-precipitation modelling (*Continued*).

No.	Reference	Model Equations	Notation
7	Maurer *et al.* (1999)	$\frac{dX_P}{dt} = k_P f_i m_i f_j m_j K_P \left(K_{PPT} + \frac{X_P}{X_{TS}}\right)^{-1}$	where • X_P is the mineral precipitate; • m_i and m_j are the concentrations of soluble ionic components; • k_P is a kinetic constant for precipitation; • K_P is the hyperbolic coefficient; • X_{TS} is the conentration of total solids; • f_i and f_j are the activity coefficients.
9	Shaojun and Mucci (1993)	$R = R_f - R_b = k_f (\gamma_i m_i)^{n_1} (\gamma_j m_j)^{n_2} - k_b$	where • R_f and R_b are the forward and backward reaction rates; • k_f and k_b are the forward and backward rate constants; • m_i and m_j are the concentrations of ionic components; • γ_i and γ_j are the activity coefficients of the components; • n is the reaction rate order.

were assigned to all the equilibria followed by an approximation of the coefficients by a set of quadratic equations. Once the quadratic equations were set and solved, the next step involved the estimation of PO_4^{3-} using the charge balance (electroneutrality) of the system. Consequently, the system of equations was solved for other species, checked for consistency and the range and output plotted. The authors argued the importance of a theoretical estimation to guide further laboratory and field experimentation.

Equilibrium calculation programs have also been used to study precipitation. These programs calculate the equilibrium composition based on equilibrium constant approach. A new method to predict struvite potential in AD systems was developed by Ohlinger *et al.* (1998). This method included the ionic strength, ionic activities, magnesium phosphate complexation effects on ion speciation and the experimentally determined struvite solubility constant. The method was verified using *MINEQL+*. *MINEQL+* was used to calculate a set of theoretical equilibrium concentration values for ions and complexes present in the system. Theoretical total magnesium, total ammonia, and total phosphorus concentrations were calculated. The measured theoretical concentrations and variances from lab tests were used to produce an objective function. The objective function was minimized to arrive at a solubility constant, $pK_{SP} = 13.26$ for struvite.

The thermodynamic approach to quantify precipitation in aqueous environments generally involves the prediction of the equilibrium composition of the system at a given point in time. Such a method does not provide information about the dynamics of the species or components taking part in the precipitation reaction. Additionally, studies based on thermodynamic approach did not take into account the biological processes taking place in the system. Hence, the influence of the biological processes, in terms of pH, on precipitation and vice-versa was largely neglected.

Some studies (Barat *et al.*, 2011; Mbamba *et al.*, 2015a,b) adopted a method in which the thermodynamic and kinetic approaches were combined to model the system. In practice, some of the reactions were described by adopting the equilibrium approach whereas others processes were kinetically solved. Such a choice largely depends on the process being modelled and the precipitation reaction under study. More often, protonation/deprotonation reactions are modelled as equilibrium based while slow precipitation reactions are kinetically controlled. For instance in Barat *et al.* (2011), a calcium phosphate precipitation model was incorporated into the Activated Sludge Model No.2 (ASM2d). The model considered two types of reactions resulting in precipitation of calcium phosphate. The aqueous phase reactions (fast) and ion-paring reactions were modeled as equilibrium reactions by adopting the equilibrium approach, while the aqueous to solid-phase reactions (slow) were kinetically modelled. A surface-based kinetic was considered for precipitation reactions (solid phase). The use of a complete kinetic approach would have required one differential equation per species (28 in total), while the use of the equilibrium approach

reduced the problem to 7 differential equations, one for each of the component, thus increasing the computation efficiency.

Over the course of years, full kinetic models evolved as well. The kinetic method of estimating the precipitation of mineral phases in wastewater systems assumes all the physicochemical reactions in the system as kinetic reactions in a dynamic state equation set. This set of differential equations is solved with respect to the variables describing the system. With such a method, the time varying nature of the species and components can be effectively traced and used to set up a decision-making strategy. For example, a dynamic model was formulated by Maurer & Boller (1999), based on the experimental observations that, in inactivated sludge containing high amounts of dissolved calcium and phosphorus, a pH-sensitive and reversible precipitation process exists. The model described the calcium and phosphate precipitation by using protonation/deprotonation reactions of phosphoric acid, carbonic acid and water. It also included fully reversible precipitation of hydroxydicalcium phosphate ($Ca_2HPO_4(OH)_2$, HDP) and formation of hydroxyapatite ($Ca_5(PO_4)_3OH$, HAP) from HDP. HAP is considered to be a stable product. All the reactions in the system were kinetically modeled. This approach was preferred because the effluent concentrations of the waste treatment plants are generally modeled as dynamic state variables.

The first and foremost attempt to model the three phases of an AD system, in the context of mineral precipitation, came from Musvoto *et al.* (2000a, b). In this study, a kinetic model for the carbonate system was developed. Ion-pairing and precipitation reactions were included in the model to describe chemical changes due to the formation of struvite, newberyite, amorphous calcium and magnesium carbonate. Further, stripping of CO_2 and NH_3 was considered. Aqueous phase mixed weak acid/base chemistry and ion-pairs constituted the ion-pair module. This was achieved by implementing a similar kinetic model for both the association/dissociation acid/base reactions and the equilibria of ion-pair formation. The aqueous phase weak acid/base submodule involved water, carbonate, phosphate, short chain fatty acid and ammonium. In total, 15 components and 26 processes were defined to implement the aqueous phase weak acid/base submodule. Likewise, to implement the ion-pair submodule, a total of 12 compounds and 22 processes were used. Here it should be noted that the forward reaction rate for ion pair formation was selected to be very high ($10^7\ s^{-1}$) and the reverse rate was calculated subsequently from the stability constant values. As mentioned earlier, the model also included a sub-module for multiple mineral precipitation. Attention was given to magnesium, calcium and few other relevant minerals. Four possible magnesium phosphates ($MgNH_4PO_4 \cdot 6H_2O$, $MgHPO_4 \cdot 3H_2O$, $Mg_3(PO_4)_2 \cdot 8H_2O$, $Mg_3(PO_4)_2 \cdot 22H_2O$), five calcium phosphates ($Ca_5(PO_4)_3OH$, $Ca_3(PO_4)_2$, $Ca_8(HPO_4)_2(PO_4)_4 \cdot 5H_2O$, $CaHPO_4$, $CaHPO_4 \cdot 2H_2O$) and other minerals ($MgCO_3 \cdot 3H_2O$) were considered. A concentration-based kinetic rate formulation was used with a default

order of reaction of 2. Solubility product values were modified according to the Debye-Hückel rule for low and medium saline waters. The solubility product values did not consider the temperature variation. Calibration and validation of the model was carried out by experimental batch results from a spent wine upflow anaerobic sludge bed (USAB) digester and a sewage sludge digester. Further, experimental values from literature were also used to fit the model simulations. The model was implemented on the *AQUASIM* platform (Reichert 1994). The quantitative estimation of precipitation of carbonates and phosphates as well as the amount of CO_2 and NH_3 stripping from the digester was justified.

In a recent study (Mbamba *et al.*, 2015a), a set of detailed experiments to support a precipitation modelling approach was carried out. The modelling approach was applied to the case of calcite precipitation. The model was designed keeping in mind the adaptability to *Generalized Physicochemical Modelling Framework* (Batstone *et al.*, 2012). Furthermore, the authors discussed possible usable control strategies and nutrient recovery models. pH titration tests and constant composition experiments were carried out to define the base line of the model approach and then deduce the environmental factors on the baseline, respectively. Ion-pairing and acid-base reactions were formulated algebraically following the mass action principle. Parameters from thermodynamic databases were used to formulate correct stoichiometry and to assign appropriate equilibrium constants to the chemical reactions. Chemical activities of each component were also considered by multiplying for a correction factor. Davies equation with temperature correction was used to derive the activity coefficients. The pH was predicted by proton balance method, which considers calculations of total hydrogen using a Tableau method. The resulting algebraic equations were solved iteratively by the Newton-Raphson method. Further, precipitation and dissolution of the chemical constituents were considered based on the Saturation Index S_I approach. This approach necessitates the use of predefined conditions based on supersaturation to select or omit a given chemical precipitation reaction. For example, formation of $CaCO_3$ can be considered in the model if the saturation index reaches a value which supports formation of precipitate. In general, three conditions were used: $S_I < 0$, $S_I = 0$ and $S_I > 0$. The semi-empirical precipitation kinetics was based on total dissolved calcium ($S_{Ca^{2+}}$), total dissolved carbonate ($S_{CO_3^{2-}}$) and total particulate calcium carbonate (X_{CaCO_3}). It is important to note that CO_2 stripping was not considered in the model. The reason suggested by the authors corresponds to the low availability of inorganic carbon in liquid phase. This was entrapped by the addition of NaOH which caused little to no stripping of CO_2. The predictions of the aqueous phase model were compared with *Visual MINTEQ* (Version 3.0, Royal Institute of Technology (KTH)). The set of algebraic and ordinary differential equations were solved using an ODE solver and the Newton-Raphson method.

A general methodology to include physicochemical processes in multiphase wastewater treatment models under a plant-wide modelling framework was

developed in (Lizarralde *et al.*, 2015). The model emphasized the definition and selection of biochemical, chemical and physicochemical processes taking place in a multiphase environment. The physicochemical plant-wide modelling methodology involved: (1) the definition of the model components and transformations; (2) the mass-transport definition for a multiphase model of wastewater treatment plant; and (3) the numerical solution procedure. The first step in this methodology, demands the compilation of the biochemical, chemical and physicochemical processes. This was achieved by denominating and specifying the relation between: (1) COD, N, P or S removal to biochemical model; (2) acid-base equilibrium and ion-pairing equilibrium to chemical model; and (3) liquid-gas transfer and liquid-solid transfer to physicochemical model. Subsequently, important transformations were individuated and introduced in the model by means of relations between dynamic state variables. The liquid-solid transfer processes involved precipitation and dissolution processes. The major precipitates were defined and included in the model. They include $CaCO_3$, $MgCO_3$, $Ca_3(PO_4)_2$, struvite, k-struvite and newberyite. A kinetic model based on ion activity product (IAP) was reformulated to take into account the spontaneous nucleation in addition to the development of supersaturation, nucleation and growth of the solids. Interestingly, dissolution was considered as the reverse of precipitation process, which made it easier to implement. The ion-pairing processes in the chemical model are built at the end in conjugation with acid-base equilibrium processes. The relevant chemical components and species were selected and represented as generic dissociation reactions. The chemical equilibrium could be solved through ordinary differential equations or by algebraic equations.

5.3.1.2 ADM1-based precipitation models

Soon after the publication of ADM1, the model received a considerable amount of criticism for some errors and omissions (Batstone *et al.*, 2006; Kleerebezem & van Loosdrecht, 2006). These concern mostly the complexity of the model structure, the stoichiometry and inhibition kinetics of the biological processes, the number and the uncertainty of the parameter values. Requests were also received for the inclusion of important anaerobic processes such as sulfate reduction (Batstone *et al.*, 2006; Kleerebezem & van Loosdrecht, 2006), phosphorus metabolism and physicochemical processes (mineral precipitation in particular). These omissions were acknowledged by the authors of the model and a '*Generalized Physicochemical Modelling Framework*' was developed (Mbamba *et al.*, 2015a). However, multiple studies have been carried out with modified versions of ADM1. These studies include extensions for both biochemical (Federovich *et al.*, 2003; Galí *et al.*, 2009; Parker & Wu, 2006; Peiris *et al.*, 2006) and physicochemical processes (Batstone & Keller, 2003; Flores-Alsina *et al.*, 2016; Maharaj *et al.*, 2018; Zhang *et al.*, 2015). Here we discuss the ADM1 extensions to include precipitation processes.

Calcium carbonate ($CaCO_3$) precipitation was implemented as a minor structural modification to the standard ADM1 (Batstone & Keller, 2003). To predict $CaCO_3$ precipitation, three additional state variables ($S_{CO_3^{2-}}$, S_{Ca} and S_{CaCO_3}) representing the concentrations of CO_3^{2-}, Ca^{2+} and $CaCO_3$ respectively, were defined and added. Simple first-order kinetic rate equations for HCO_3^-/CO_3^{2-} acid-base reactions and $CaCO_3$ precipitation reaction were also added. ΔH° values of precipitation and acid base reactions were used to calculate the change in value of the equilibrium coefficients due to temperature. The model was used to assess two case studies: (1) recycled paper-mill wastewater fed to UASB, and (2) gelatine production wastewater fed to solids digester.

A more detailed physicochemical framework was implemented by (Zhang *et al.*, 2015) to simulate the dynamics of calcium caonate ($CaCO_3$), magnesium carbonate ($MgCO_3$), struvite ($MgNH_4PO_3$), magnesium phosphate ($MgHPO_4$) and tricalcium phosphate ($Ca_3(PO_4)_2$). ADM1 was modified by improving the biochemical framework and integrating a more detailed physicochemical (gas transfer and precipitation) framework. The changes in inorganic carbon and nitrogen for decay processes were considered and carbon and nitrogen balances were closed by adding balance terms of inorganic carbon and nitrogen for the microbial decay processes. Two balance terms based on a previous study (Blumensaat & Keller, 2005) were introduced into the original ADM1 to resolve the discrepancies between carbon and nitrogen contents in the degraders and substrates. In the physicochemical framework, an additional gas transfer process was incorporated to account for NH_3. Further, inorganic components for acid-base reactions and solid precipitation were added. The inorganic carbon components included dissolved carbon dioxide, bicarbonate and carbonate. Similarly, inorganic phosphate components such as phosphate, hydrogen phosphate, dihydrogen phosphate and phosphoric acid were introduced into the model. Consequently, the charge balance was modified to accommodate the new components. A second-order irreversible precipitation model was used to improve the ability of the model to simulate non-biologically mediated processes. The model equation used in this study is based on the fundamental relation for crystallization process which can describe precipitation processes better than any simple first-order rate equations based on pseudo-equilibrium. The model was validated with literature data. The model was used to assess the effect of calcium ions, magnesium ions, inorganic phosphorus and inorganic nitrogen on a batch anaerobic digester.

A series of model extensions, aimed at improving the interactions of phosphorus, sulfur and iron, mineral precipitation processes, were implemented in the framework of ADM1. The extended ADM1 was the part of a larger plant-wide model. The model extension (A_3) included: (1) aqueous chemistry model (Solon *et al.*, 2015), and (2) a multiple mineral precipitation model, MMP (Mbamba *et al.*, 2015b). The first submodule estimates the pH by considering ionic behaviour of non-ideality (ion-pairing and ion activity) instead of molar ion concentration. A set of non-linear algebraic equations were used to resolve the aqueous chemistry

module. The method includes: (1) Davis equation based ionic strength correction; (2) ion-pairing equilibrium reactions for inorganic carbon, inorganic nitrogen and VFA; and, (3) multi-dimensional Newton-Raphson method to solve the set of algebraic equations. In the second submodule of MMP, a reversible mechanism of precipitation has been implemented using saturation index. This methodology of predicting precipitation reactions has been already explained in detail (Mbamba *et al.*, 2015a, and Section 5.3.1.1). The MMP model simulates the dynamics of calcite (X_{CaCO_3}), agronite ($X_{CaCO_{3a}}$), amorphous calcium phosphate ($X_{Ca_3(PO_4)_2}$), hydroxylapatite ($X_{Ca_5(PO_4)_3(OH)}$), octacalium phosphate ($X_{Ca_8H_2(PO_4)_6}$), struvite ($X_{MgNH_4PO_4}$), newberyte (X_{MgHPO_4}), magnesite (X_{MgCO_3}), k-struvite (X_{KMgPO_4}), iron sulfide (X_{FeS}.), iron phosphate ($X_{FePO_4}/X_{Fe_3(PO_4)_2}$), and aluminium phosphate (X_{AlPO_4}).

Recently, a model based on ADM1 has been proposed which explicitly predicts the dynamics of TEs (Fe, Co and Ni) in terms of mineral precipitation in an anaerobic batch reactor (Maharaj *et al.*, 2018). In the biochemical module, the microbial uptake of TE and the TE inhibition on microbial activities have been introduced. A dose response function has been implemented to model the effect of TEs on anaerobic production of methane. The function considers deficiency, activation, inhibition and toxicity of TEs on the microbial groups. In the physicochemical module, ion association/dissociation reactions and liquid-gas transfer reactions are considered for liquid-liquid processes and liquid-gas processes, respectively. Equilibrium reactions are modeled by a set of differential equations. The incorporation of the precipitation reactions in the physicochemical module leads to the definition of new inorganic components in the ADM1 framework. The model takes into consideration inorganic carbonate (e.g. CO_2, HCO_3^- and CO_3^{2-}), inorganic phosphate (e.g. PO_4^{3-}, HPO_4^{2-}, $H_2PO_4^-$ and H_3PO_4) and inorganic sulfide (e.g. HS^- and S^{2-}) components in liquid phase. The components of the three chemical systems (carbonate, phosphate and sulfide) react, in the liquid phase, to form precipitates (e.g. $CoCO_3$, $Co_3(PO_4)_2$, FeS, FeS, $FeCO_3$, $Fe_3(PO_4)_2$, $NiCO_3$, $Ni_3(PO_4)_2$, NiS, $MgNH_4PO_4$), whose formation is governed by the K_{sp} values. A full kinetic framework has been used to implement the precipitation process. The model was implemented on an original code in MATLAB platform and has been solved using 'ode15s' routine. The model was used to study the effect of changes in the initial concentration of sulfur and phosphorous, the effect of nutrient starvation on methane production and the dynamics of TEs in AD.

5.3.2 Adsorption

Adsorption of TEs in AD can proceed through three different mechanisms: (i) adsorption of TEs on precipitates forming in the digester; (ii) complexation of TEs on organic matter released by the microorganisms; and (iii) adsorption of TEs on the surface of the microorganisms. In the first case, when a precipitate

is formed it provides many adsorption sites for various cations and anions. In the second and third case, various carboxylic and amino groups of organic surfaces provide sites for the surface complexation of TEs. In general, TE adsorption in biogeochemical systems has been studied and reviewed to a great extent (Konhauser, 2007; Warren & Haack, 2001). However, only few attempts to model the adsorption process in wastewater treatment systems exist in literature (Hauduc *et al.*, 2015), and up to date they have not been implemented in the ADM1 framework to study the effect of TEs adsorption on AD performance. In the following section, we report the modelling efforts to simulate the adsorption process in wastewater environments. For a general overview of the models adopted for biosorption the reader can refer to Papirio *et al.* (2017).

The general strategy to model adsorption processes is derived from geochemical reaction modelling techniques. In this approach, a chemical equilibrium problem is formed comprising the major chemical reactions taking place. Further, the equations are solved simultaneously by the Newton-Raphson algorithm. The equilibrium constants of the individual reactions within the system are of major importance because such models consider every physicochemical reaction as being in equilibrium. For example, the mechanisms behind the chemical-mediated phosphorus system was studied in (Smith *et al.*, 2008). The study was aimed at investigating the major factors affecting phosphorus removal and also the effect of various operational parameters. The model took into consideration all the possible surface reactions on hydrous ferric oxide. The basis of the model is that iron and phosphorus share an oxygen atom. The chemical equilibrium problem was divided in two parts for numerical reasons. The first part solves or quantifies the thermodynamically-favored solid precipitates formed ($Fe(OH)_{3(s)}$ and $FePO_{4(s)}$). Once the precipitated solids are estimated, a second calculation step is performed solving a second equilibrium problem where phosphate is allowed to complex with active sites (adsorption sites) on the precipitated hydrous ferric oxide (HFO). As the authors pointed out, phosphate removal should be considered with phosphate precipitation. However, the surface complexation modelling formalism was adopted in this case to remove phosphate from the system in the earlier reaction step (hydrolysis). This was done by kinetically linking the process to the mixing.

In other cases, the kinetic approach to model the adsorption process in a wastewater system has been adopted. In such case, the adsorption of a chemical species is considered to be kinetically controlled. The kinetic approach to define the physicochemical system is easier to implement because in most of the biochemical framework, AD models are kinetically controlled rather than equilibrium controlled. The process of chemical phosphorus removal in wastewater was kinetically modelled by (Hauduc *et al.*, 2015). Such dynamic model serves as a tool to optimize chemical dosing, taking into consideration the effluent phosphorus concentration due to regulatory reasons. The model predicts the stoichiometry and kinetics of precipitation of hydrous ferrous oxides

(HFO), phosphate adsorption and co-precipitation. Thus, chemical equilibrium dissociation, chemical ion pairing, physical mineral precipitation process, chemical surface complexation, and aging of precipitates were considered in the model. Kinetic models used for adsorption processes in wastewater treatment are limited to pseudo-first-order rates (Lagergren type). The adsorption equation expresses the variation of component concentration as function of a driving force which is the difference between the amounts of the component that should be bound at equilibrium. This is calculated based on the equilibrium constants and actual bonded component. For monodentate and bidentate species the order of the reaction is one and two, respectively. The adsorption sites on the flocs are not equally accessible to phosphorus. More accessible sites are available first, which reduces in number with the course of adsorption. Therefore the rate of adsorption decreases. This decrease in kinetic rate due to a decrease in accessibility of remaining sites have been modeled by multiplying the ratio $(\mathrm{SiteF}/\mathrm{SiteT})^n$ to the overall rate, where, n is 1 for monodentate and 2 for bidentate species. The ratio is the amount of free sites (SiteF) to the amount of total sites (SiteT) with a value between 0 and 1.

A biogeochemical framework (CCBATCH) was implemented and expanded by adding surface complexation reactions to the already developed biodegradation and chemical equilibrium sub models (Schwarz & Rittmann, 2007). The surface complexation sub-model included both electrostatic and non-electrostatic surface complexation reactions. Metal complexation by active cells, inert biomass (solids) was described by the electrostatic surface complexation model. The non-electrostatic sub-model was used to describe metal complexation reactions of extracellular polymeric substances (EPS) and biomass-associated-product (BAP). The model assumed a negative charge on the surface of the cell which is due to the protonation/deprotonation of carboxyl, phosphoryl and hydroxyl groups. The interaction of these negatively charged surface species with the adsorbing protons was quantified according to the capacitance model of microbial surface. Further, to understand the biological and non-biological ligand interaction with cell surface leading to metal detoxification a three-step procedure was adopted. Stoichiometry and kinetics of production of reactive ligands by the microbes were mentioned in the first step. In the second step, reactivity of the ligands towards metal was described which indirectly described the speciation of the metal in the system. Lastly, expanded CCBATCH was used to carry out titration reactions simulations. The biogeochemical analyses emphasized the fact that over various organic and inorganic microbial products, sulfide is a major promoter for Zn detoxification. It was shown that, in presence of sulfide, detoxification of Zn occurs while in absence of sulfide, Zn complexes with biogenic organic ligands providing a mechanism for detoxification.

A surface-complexation modelling approach to describe the metal ion interactions with microbial surface has also been studied in (Daughney & Fein, 1998). This

modelling technique makes use of stability constants to model metal-microbial surface interaction. However, stability constants for metal-microbial surface complexes, which form the backbone of this modelling technique, are rarely reported because of the intricacies of the experimental methods involved in their determination. Therefore, the stability constants were predicted using a linear free energy approach. In this regard, measured microbial metal-carboxyl stability constants are related to stability constants for aqueous metal-organic acid anion complexes that involve the same metal cation. If the correlation between these two types of stability constants is valid, an unknown value for a metal-carboxyl microbial surface stability constant can be estimated provided the stability constant for the metal-organic acid anion aqueous complex is known. Whether such a relationship could be constrained for a widely studied organic acid anion, it would provide a means of estimating the microbial adsorption behavior of a wide range of metal cations.

5.3.3 Aqueous complexation

Anaerobic digestion is rich in organic matter. The organic matter is composed of biomass, humic substances and other organic molecules from the biodegradation, such as VFAs, alcohol and acetate. Their formation is one of the major biochemical reactions in AD. These organic substrates and humic substances act as chelating agents affecting metal speciation. Thiol-containing organic matter, as represented by cysteine, has also been reported to take part in aqueous complexation with TEs as a strong functional group (Yekta *et al.*, 2014a, b). Additionally, in the course of AD, synthetic chelating agents are occasionally added to improve the digester performance. Synthetic agents, such as EDTA, influence (imparting both positive and negative effects) the bioavailability of TEs in AD by forming stable soluble complexes. Thus, three groups of organic species should be taken into consideration for organic complexation modelling: (1) organic substrates in AD (for example, VFAs); (2) humic substances; and (3) synthetic chelating agents (EDTA/NTA/EDDS). Here we discuss the general methodology developed in (Willet & Rittmann, 2003) and adopted in (Maharaj *et al.*, 2019) to model TEs complexation in the ADM1 framework.

The formation and dissociation of TE complexes follows a kinetically controlled approach. The complexation reaction involving organic ligands and TEs was used here to illustrate the kinetic framework to model complexation reactions. New state variables representing the organic ligand acid/base system and complexes have to be taken into account to predict the pH of the system. The general mechanism of complexation reactions and modelling can be written as follows:

$$Me^{x} + L^{y} \xrightarrow{k_1} [MeL]^{x+y} \tag{5.20}$$

$$[MeL]^{x+y} \xrightarrow{k_{-1}} Me^{x} + L^{y} \tag{5.21}$$

where k_1 is the $[MeL]^{x+y}$ formation rate constant in $[ML^{-3}\,T^{-1}]$; k_{-1} is the dissociation constant in $[T^{-1}]$. Equations (5.16) and (5.17) can be rewritten as:

$$Me^x + L^y \overset{K_{[MeL]^{x+y}}}{\longleftrightarrow} [MeL]^{x+y} \tag{5.22}$$

where $K_{[MeL]^{x+y}}$ is the equilibrium constant for $[MeL]^{x+y}$ in $[ML^{-3}]$. The rate of change of complex over time may be written as:

$$\frac{d[MeL]^{x+y}}{dt} = k_1[Me^x][L^y] - k_{-1}[MeL]^{x+y} \tag{5.23}$$

where $[Me^x]$, $[L^y]$, $[MeL]^{x+y}$ are the dynamic state variables for the free TE concentration, organic ligand and TE-organic complex respectively. The formation rate constant, k_1, for all the species and the dissociation rate constant, k_{-1}, can be calculated from the stability constant by a simple relation as:

$$K_{[MeL]^{x+y}} = \frac{k_1}{k_{-1}} \tag{5.24}$$

5.4 MODELLING THE EFFECT OF TEs ON BIOKINETICS

5.4.1 Modelling the biouptake of TEs

It is widely accepted that metal geochemistry and environmental conditions in an engineered system affect the uptake of TEs by microorganisms (Hudson, 1998; Jansen, 2004; Sunda & Huntsman, 1998; Worms *et al.*, 2006). The bioavailability of metals in the case of AD has been recently studied (Gustavsson, 2012; Jansen, 2004; Yekta *et al.*, 2016). Bioavailability is thought to depend on: (i) the internalization pathway; (ii) specificity of metals to the transporters; (iii) physicochemistry of the bulk phase; (iv) size and nature of microorganisms; (v) concentration of metal; and (vi) metal speciation.

To effectively affect the biochemical systems, the required metals have to be transported from the bulk solution into the Cytosol (Figure 5.3). In this process metals diffuse through the external medium to the surface of the organism, they are subsequently adsorbed to the microbial surface and later internalized by the corresponding mechanisms. These transport processes control the overall metal bio-uptake rates (Jansen, 2004; Koster & Leeuwen, 2004; Worms *et al.*, 2006). The binding of metals to the surface of the microorganisms are thought to be carried out by the extracellular polysaccharides (Bhaskar & Bhosle, 2006; d'Abzac *et al.*, 2010; Malik, 2004; Loaec *et al.*, 1997). Therefore, the rate of extracellular polysaccharide formation on the microorganisms might be linked to the presence of a certain amount of a particular metal in the surrounding environment (Aquino & Stuckey, 2004). The surface-bound metals are destined to be internalized, accumulate on the surface or dissociate back to the bulk phase (Worms *et al.*, 2006). The internalization of metals depends largely on the transport system (Hudson, 1998; Jansen, 2004; Worms *et al.*, 2006). The

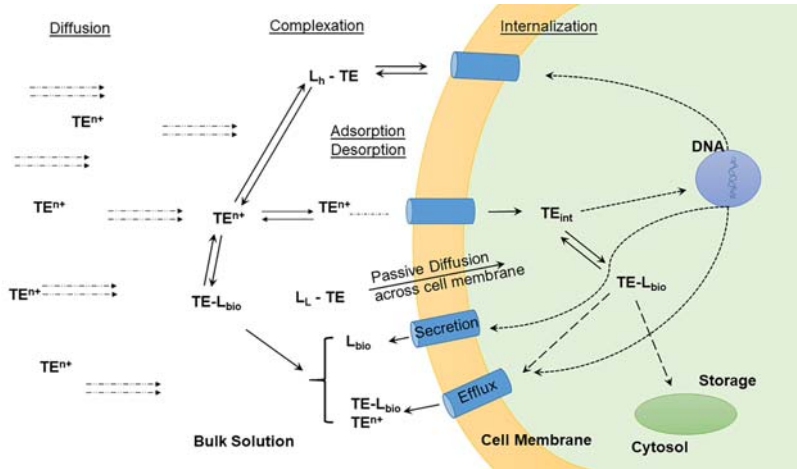

Figure 5.3 Various physico-chemical and transport mechanisms affecting TE internalization in a microbial cell. L and TE^{n+} refer to ligand and free trace element respectively. Subscripts int: internalized; bio: microbial; h: hydrophilic; L: lipophilic (adapted from Worms *et al.*, 2006).

hydrophobic nature of biological membranes limits the movement of molecules by passive diffusion. Only neutral and non-polar molecules move across the membrane by passive diffusion. Difference in concentration gradient across the membrane is the driving force for passive diffusion of molecules across the membrane. Metal species in AD are generally hydrophilic in nature and their transport is mediated by specific metal-binding proteins (Worms *et al.*, 2006). For example, metals are transported as metal ions involving ATPases, natural resistance associated microphage proteins and zinc-regulated or iron-regulated transporter. These two steps of metal binding to the surface and metal internalization by specific transporters have been expressed by Michaelis-Menten kinetics (Jansen, 2004). Further, the mass balance for total TE has been established. Starting with the case of growth limitation, metal concentration in the bulk phase can be related to growth by Monod kinetics. As Monod kinetics assumes the external metal concentration in the bulk phase, it might become erroneous to model internal metal concentration. Droop model of relating internal metal concentration to the growth renders an option here (Droop, 1983; Jansen, 2004). Microbial growth rate was defined as:

$$\frac{dx}{dt} = \mu x \tag{5.25}$$

where, μ is the growth rate constant, t is the time, and x is the biomass concentration. The limitation of growth rate due to substrate and available metal ions was

represented as follows:

$$\mu = \mu_{max} \frac{C_{MeOH}}{C_{MeOH} + K_{MeOH}} \frac{(Q_{Co} - Q_{Co,min})}{Q_{Co}} \frac{(Q_{Ni} - Q_{Ni,min})}{Q_{Ni}} \quad (5.26)$$

where μ_{max} is the maximum growth rate constant, C_{MeOH} is the primary substrate concentration, K_{MeOH} is the substrate Monod constant, Q_{Co} is the cobalt content; $Q_{Co,min}$ is the minimum Co content, Q_{Ni} is the Ni content and $Q_{Ni,min}$ is the minimum Ni content. The competition of metal ions for the same transporter was taken into account through the uptake flux rate as follows:

$$J_{Co,in} = J_{max} \frac{C_{Co^{2+}}/K_{JM,Co^{2+}}}{(C_{Ni^{2+}}/K_{JM,Ni^{2+}}) + (C_{Co^{2+}}/K_{JM,Co^{2+}}) + 1} \quad (5.27)$$

where J_{max} is the maximum uptake flux; $K_{JM,Co^{2+}}$ is the Co Michaelis-Menten constant, $K_{JM,Ni^{2+}}$ is the Ni Michaelis-Menten constant, $C_{Co^{2+}}$ is the free Co^{2+} concertation, and $C_{Ni^{2+}}$ is the free Ni^{2+} concentration. The excretion of metal ions was modelled as a first order process as follows:

$$J_{Co,eff} = k_{eff,\,Co}(Q_{Co} - Q_{Co,eff,min}) \quad (5.28)$$

where $k_{eff,Co}$ is the efflux rate constant and $Q_{Co,eff,min}$ is a threshold value below which no efflux takes place. The mass balances were established based on the above-mentioned rates. The mass balance for metal content of the cells was represented as follows:

$$\frac{dQ_{Co}}{dt} = J_{Co,in}(t) - J_{Co,eff}(t) - \mu(t)Q_{Co}(t) \quad (5.29)$$

The amount of total dissolved metal was accounted for with the following mass balance:

$$\frac{dQ_{Co,total}}{dt} = -(J_{Co,in}(t) - J_{Co,eff}(t))x(t) \quad (5.30)$$

5.4.2 Dose-response modelling of TE effect in AD

Elements in trace amounts such as Fe, Zn, Ni, Co, Mo, Cu, Mn, Se, Mo, W, and B considerably affect biogas production in anaerobic digesters by stimulating and enhancing microbial activity (Choong *et al.*, 2016; Federation, 2014; Feng *et al.*, 2010; Fermoso *et al.*, 2009; Oleszkiewicz & Sharma, 1990; Romero-güiza *et al.*, 2016). Optimal levels of TEs should be maintained by adding externally the appropriate micronutrients, especially when the feedstock used for AD is deficient in these elements. It is a common industrial practice to supply these elements externally to ensure that these will be in bioavailable form to cover the nutritional needs of the microorganisms in the anaerobic environment. However, increased concentrations of the same elements can act as inhibiting or toxic factor and result in a reduced biogas production or complete reactor

failure (Feng *et al.*, 2010; Hickey *et al.*, 1989; Lin, 1992). Working within the optimum concentration range is required to secure balancing between deficiency and toxicity and ensure minimum operating cost for additives supply. This behaviour is conceptually presented in Figure 5.4(a) for an essential TE. When an element is considered 'non-essential' for microbial growth, the deficiency part of Figure 5.4(a) is narrowed or supressed. In such cases, the effect of the element on the microbial growth presented conceptually in Figure 5.4(b) can be observed. Mathematically, this behaviour is approached by dose-response models. These models are extensively used in pharmacokinetic (PK) studies (Zhao & Yang, 2014), where the effect of dosing a medicine to a sample population is monitored by measuring some physiological response. The same concept can be applied for modelling the effect of TEs on the biological activity in anaerobic digesters.

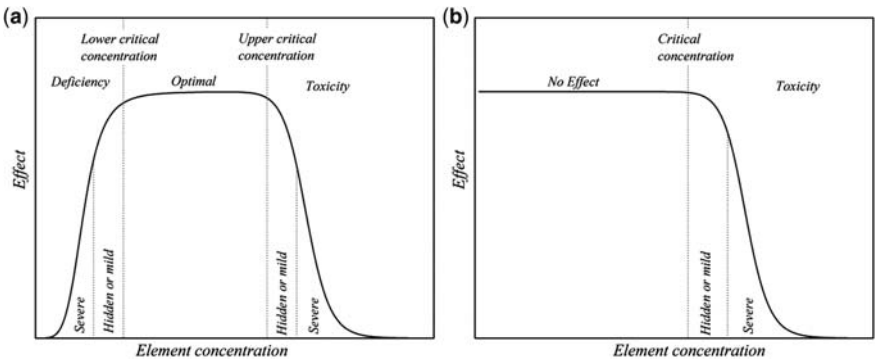

Figure 5.4 A conceptual dose-response curve for (a) an essential and (b) a non-essential element.

In typical dose response studies only the part of the response up to the maximum effect level is modelled (left hand side of Figure 5.4(a)). A sigmoidal curve usually adequately describes this part of the curve. A number of mathematical expressions simulate such a sigmoidal response. Selecting the appropriate model depends on the following aspects.

Theoretical basis of the model: Very few sigmoidal models are derived from a theoretical analysis of the dose-response effect. The majority of the models are empirical equations or mathematical expressions sharing sigmoidal curve characteristics.

Number of parameters in the model: The number of parameters affects the shape (steepness) and position of the reflection point of the sigmoidal curve. It usually ranges from two to five (excluding y_0 and y_{max} values). Equations with fewer parameters are preferred for simplicity. For the case of simple models with only two parameters, the linearized form of the equation can be used to determine the

best-fit values simulating an experimental set of data. Generally this procedure is carried out by nonlinear regression analysis.

Position of the reflection point: The position of reflection point of the sigmoidal curve is also a significant criterion to select a dose response model for simulation. The reflection point can be either fixed positioned at 50% of effective dose (ED_{50}) (e.g. $E_{\max}$ model) or parametrically adjustably above or below ED_{50}.

The concept of dose-response modelling can be directly applied in modelling the effect of TEs in anaerobic digesters. The effective concentration applied for each TE should be mathematically correlated with the induced response in the system. Therefore two critical parameters should be defined: (a) which is the selected response and at which time should the system be sampled (observed y values), and (b) which effective concentration of the TE produces a certain level of response (measured x values). Ideally, direct effects such as increased microbial activity related with higher observed growth rates and/or increased yield coefficients should be quantified experimentally. Microbial growth rate expressions can be modified appropriately by including terms for the effect of TEs. When Monod kinetic expressions are used, these can be modified as follows:

$$r_i = \mu_{\max,i} \frac{S_i}{K_i + S_i} \cdots \frac{S_j}{K_j + S_j} \ldots f(I_i) \ldots f(I_j) \ldots f(pH) f(T) \ldots f(TE_i) \ldots f(TE_j) \tag{5.31}$$

where r_i is the specific growth rate of microorganisms in process i [ML^{-3} T^{-1}]; $\mu_{\max,i}$ is the maximum specific growth rate of microorganisms in process i [T^{-1}]; $S_i \ldots S_j$ is the concentration of limiting substrates $i \ldots j$ e.g. carbon source, nitrogen source etc. [ML^{-3}]; $K_i \ldots K_j$ is the half saturation constant for the components $i \ldots j$ [ML^{-3}]; $f(I_i) \ldots f(I_j)$ are the factors for inhibiting substances e. g. free ammonia, butyrate (dimensionless); $f(pH)$ is the effect of pH on the specific growth rate of microorganisms in process I; $f(T)$ is the effect of temperature on the specific growth rate of microorganisms in process i (dimensionless); $f(TE_i) \ldots f(TE_j)$ is the effect of TEs $i \ldots j$ on the specific growth rate of microorganisms in process i (dimensionless).

In a traditional modelling approach biomass yield (Y) and related stoichiometric coefficients are considered constant, although they may vary significantly during the growth stages of the microbial biomass and the physicochemical conditions in cell's environment (e.g. TEs). When the yield is affected by the presence of essential TEs then a similar approach can be used:

$$Y = Y_0 f(TE_i) \ldots f(TE_j) \tag{5.32}$$

where Y is the observed yield coefficient in the presence of TEs; Y_0, is the maximum yield coefficient at the optimum level of TEs; $f(TE_i) \ldots f(TE_j)$ is the dose response equations related with the TEs $i \ldots j$.

Assuming that an element is essential for growth, any sigmoidal curve describing the left hand side of Figure 5.4(a) can be used as a modifying function. The model would result in non-growth conditions when the element is absent. This corresponds to complete reactor failure due to severe element deficiency. Conditions of mild deficiency are also modeled by equations (5.27) or (5.28) at moderate element concentration. Finally, saturation is predicted when the concentration of TEs are within the optimal range. Equations (5.27) and (5.28) should be modified appropriately when the observed rates and/or yields are not bound between 0 and 1 as in a 'typical' sigmoidal curve. For example when the baseline effect is different than zero the appropriate $f(TE_j)$ functions should be used. Toxicity modelling is also possible by selecting appropriate mathematical expression such as equations in Table 5.5.

Estimating the bio-kinetic parameters for an anaerobic digester, by fitting a model to experimental data, assumes that the only limiting or inhibiting substances that affect the process are these already included in the kinetic expressions of the model (e.g. first part of equation 5.27). However under severe or mild TEs deficiency (correspondingly toxicity) the bio-kinetic estimated parameters might be significantly misleading as the system does not perform under optimum conditions. The use of an updated revised model would result in a different set of parameters that include also the effect of the trace elements in the system.

Another significant aspect which should also be addressed is the selection of the classes of the microbial consortia present in an anaerobic digester which are mostly affected by the elements deficiency. It has been shown that the microorganisms that are more sensitive to TEs fluctuation and deficiency are those belonging to the group of methanogenic archaea (Glass & Orphan, 2012). Therefore, the critical step in this modelling approach is to focus primarily on the metabolic activity of this group by modifying the appropriate kinetic expression and/or yield coefficients.

It is also important to define what is considered the effective concentration (dose) of a TE in an anaerobic bioreactor resulting to a certain level of stimulating response (or correspondingly toxicity effect). In pharmacokinetic studies when a new medicine is tested in a sample population, a prescribed amount is administered, while the resulted physiological response is monitored (e.g. changes in blood pressure). Even if the drug is distributed differently in the human organs, excreted, accumulated or metabolized, the total amount of the drug administered is considered as the effective dose. However, in those studies factors such as age, sex, race and so on, may significantly differentiate the results. Similarly, in the case of anaerobic digesters, the total concentration of trace elements could be used as a rough indication of the dose to be used in dose-response equations. However, it is realized that a significant fraction of the total element in a bioreactor is in non-readily bioavailable form and will not affect directly biogas production (Thanh *et al.*, 2015). Part of the element can be distributed according to the

Table 5.5 List of dose-response functions.

No.	Name	Dose-response Function	General Trend
1	Hill equation	$y = y_{max}\frac{x^n}{a^n + x^n}$ where • y_{max}, a are parameters of the model • n is the Hill coefficient	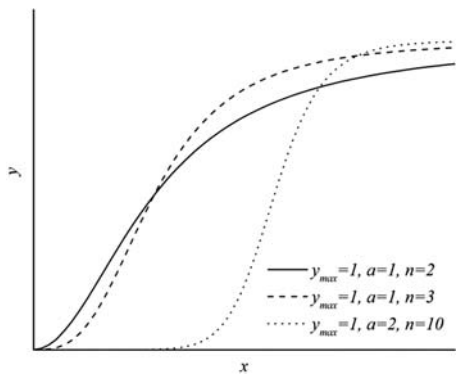
2	E_{max} equation	$y = E_0 + E_{max}\frac{D^n}{ED_{50}^n + D^n}$ where • E_{max} is maximum change in effect from base line level • E_0 is baseline effect (or placebo effect in pharmacokinetic), corresponding to the response when the dose is zero (left asymptote parameter) • ED_{50} is dose which achieves 50% of the maximum response • D is dose	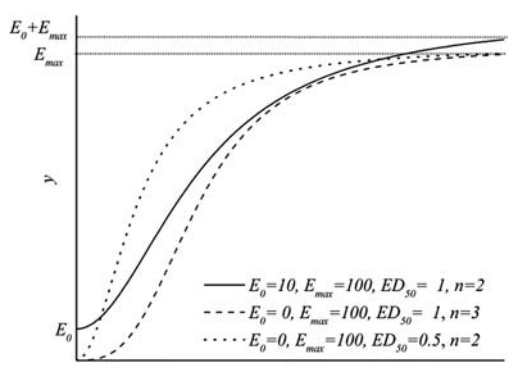

3	Logarithmic reciprocal equation	$y = e^{a-b/x}$ where • a and b are parameters of the model	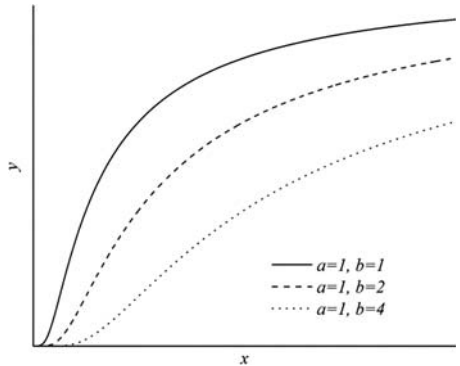
4	Logistic equation	$y = \frac{y_{max}}{1+e^{-(a+bx)}} = \frac{y_{max}}{1+a'e^{-bx}}$ where • y_{max}, a or a' and b are parameters of the model	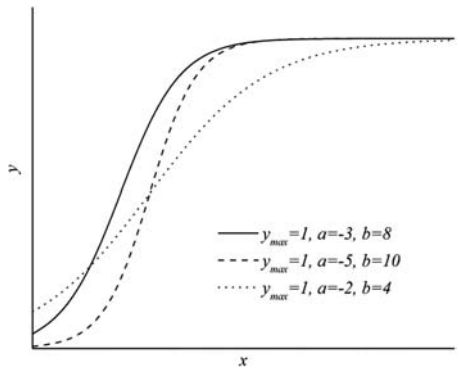

(*Continued*)

Table 5.5 List of dose-response functions (*Continued*).

No.	Name	Dose-response Function	General Trend
5	Log-Logistic equation	$y = \frac{y_{max}}{1 + ae^{-b\,ln(x)}}$ where • y_{max}, a and b are parameters of the model	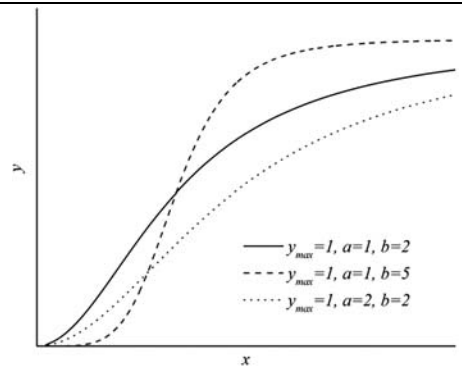
6	Gompertz equation	$y = y_{max}e^{-e^{-(a+bx)}} = y_{max}e^{-a'e^{-bx}}$ where • y_{max}, a and b are parameters of the model.	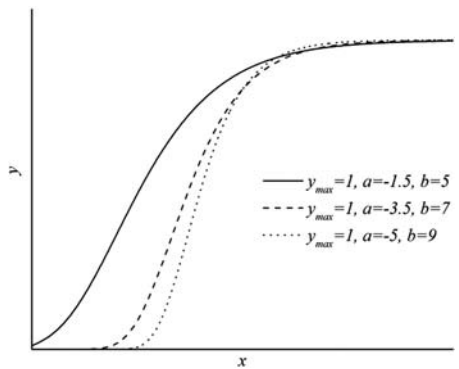

7	Weibull equation	$y = y_{max} - ae^{-bx^c}$ where • y_{max}, a, b and c are parameters of the model	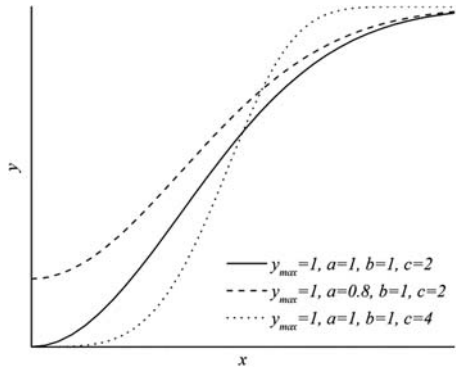
8	Richard's equation	$y = \frac{a}{(1 + e^{-(b+cx)})^d}$ where • a, b, c and d are parameters of the model	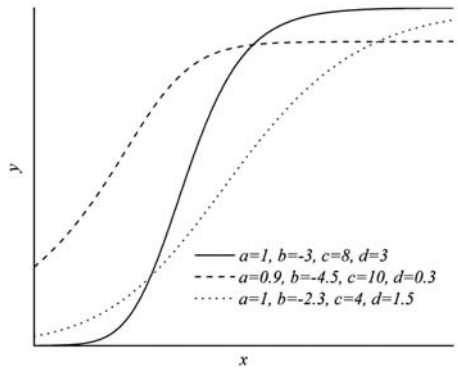

(*Continued*)

Table 5.5 List of dose-response functions (*Continued*).

No.	Name	Dose-response Function	General Trend
9	Equations simulating stimulation and toxicity effects	$y = y_0 + \frac{y_{max-y_0}}{\left(1+\frac{EC_{50}}{x}\right)^a \left(1+\frac{x}{IC_{50}}\right)^b}$ where • y is the recorded response • y_0 is the baseline of the recorded response at concentration levels approaching zero • y_{max} is the maximum observed response • EC_{50} is the concentration of trace element where 50% of the maximum effect is achieved • IC_{50} is the concentration of the element where 50% inhibition (toxicity) is observed • a and b are parameters that affect the slope of the left hand side and right hand side of the curve respectively	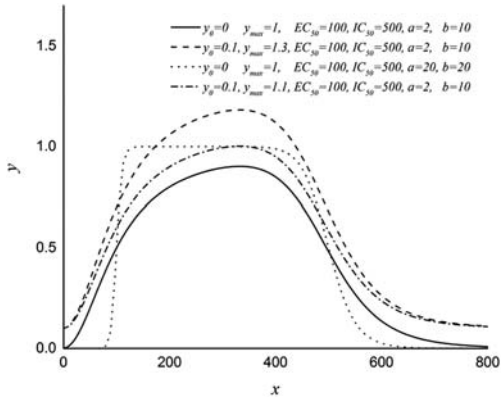
10	Equations simulating hermetic effects	$y = \frac{(x+a)}{b + c(x+a) + d(x+a)^2}$ where • a, b, c and d are parameters of the model	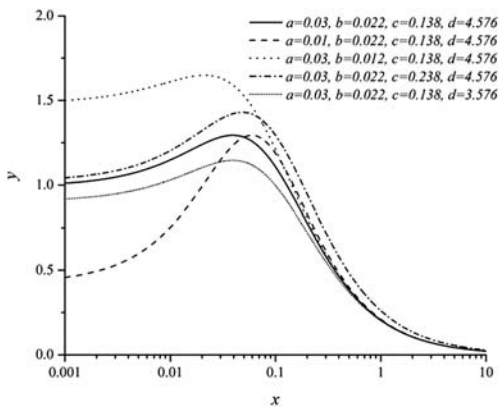

following processes (Callander & Barford, 1983a, b): reversible or irreversible adsorption on the surface of solids (Section 5.3.2); precipitation to inorganic minerals by abiotic reactions (e.g. hydroxide, carbonate, phosphate, sulfide precipitates; Section 5.3.1); volatilization of the elements that produce inorganic or organic volatile compounds (e.g. volatile selenium compounds); redox reactions that affect the solubility of the element (e.g. Cr(III)/Cr(VI), Fe(II)/Fe(III), Se(VI)/ Se(IV)/ Se(0)/ Se(-II)); complexation by organic ligands (e.g. proteins, humic acids, fulvic acids, yeast extract, EDTA, NTA, EDDS; Section 5.3.3) (Gonzalez-Gil *et al.*, 2003; Zhang *et al.*, 2015) and species distribution according to the element speciation (e.g. poly hydroxyl species) (Yekta *et al.*, 2016).

Alternatively, as a rough estimate of the effective concentration (dose) it would be appropriate to use the soluble fraction of the TE present in the reactor liquid phase. However even under this convention, metal complexes with organic macromolecules could still be in non-bioavailable form. Thus, it is of primary concern to determine which chemical species of the TE are actually considered directly bioavailable to enhanced biogas production and system stability (Yekta *et al.*, 2016).

From the mathematical point of view, inclusion of terms for TEs in an existing model unavoidably increases model complexity. For each TE a new state variable in the liquid phase should be introduced. In addition, a set of at least two new parameters should be provided to include the appropriate sigmoidal shape equation in the model. The complexity increases considerably when different species of the TE should also be included as well as speciation modelling equations to calculate the concentration of these species. These algebraic equations corresponding to the equilibrium law for each reaction usually are treated as instantaneous or fast dynamic equations. Furthermore, processes such as adsorption, complexation or precipitation of the TEs require definition of additional processes and their corresponding rates or equilibrium equations. Providing coherent initial conditions for such a complex system is crucial for the initialization of the integration algorithm. Additionally, the difference in time scales between slow biological actions and fast dynamic or equilibrium abiotic reactions results in system stiffness. This is the cause of solution failure in the propagation of a solution algorithm.

5.5 CONCLUSION

This chapter reviewed the modelling aspects describing the main processes that affect TE dynamics in AD environment. The consolidated knowledge from the literature indicates that the effect and fate of TEs in AD system can be modelled to predict the dynamic behavior of TEs in AD. However, there is a need to improve the currently available AD models to account for precipitation, adsorption, aquatic complexation and bio-uptake of TE, so as to quantify their fate and effect. While problems may arise due to increase in model complexity,

the modelling approach should be compatible with the existing AD framework (ADM1). Consequently, taking into account the multiplicity of processes that affect TE dynamics in AD systems as well as the importance of these processes in defining the biology and physicochemistry of the AD system, the need for a TE module embedded within the ADM1 model has been recognized. This sets the priorities in the efforts towards 'mathematical model-based controlled TE dosing' in engineered AD systems.

REFERENCES

Ali M. I. and Schneider P. A. (2008). An approach of estimating struvite growth kinetic incorporating thermodynamic and solution chemistry, kinetic and process description. *Chemical Engineering Science*, **63**(13), 3514–3525.

Allison J. D., Brown D. S. and Novo-Gradac K. J. (1991). MINTEQA2/PRODEFA2, a Geochemical Assessment Model for Environmental Systems: Version 3.0 User's Manual. U. S. Environ. Prot. Agency EPA/600/3-91/021 115. USEPA, Washington, DC.

Aquino S. F. and Stuckey D. C. (2004). Soluble microbial products formation in anaerobic chemostats in the presence of toxic compounds. *Water Research*, **38**, 255–266, https://doi.org/10.1016/j.watres.2003.09.031

Banerjee R. and Ragsdale S. W. (2003). The many faces of vitamin B12. *Annual Review of Biochemistry*, **72**, 209–247, https://doi.org/10.1146/annurev.biochem.72.121801.161828

Barat R., Montoya T., Seco A. and Ferrer J. (2011). Modelling biological and chemically induced precipitation of calcium phosphate in enhanced biological phosphorus removal systems. *Water Research*, **45**, 3744–3752, https://doi.org/10.1016/j.watres.2011.04.028

Barrera E. L., Spanjers H., Dewulf J., Romero O. and Rosa E. (2013). The sulfur chain in biogas production from sulfate-rich liquid substrates: A review on dynamic modelling with vinasse as model substrate. *Journal of Chemical Technology and Biotechnology*, **88**, 1405–1420, https://doi.org/10.1002/jctb.4071

Barrera E. L., Spanjers H., Solon K., Amerlinck Y., Nopens I. and Dewulf J. (2015). Modelling the anaerobic digestion of cane-molasses vinasse: Extension of the Anaerobic Digestion Model No. 1 (ADM1) with sulfate reduction for a very high strength and sulfate rich wastewater. *Water Research*, **71**, 42–54, https://doi.org/10.1016/j.watres.2014.12.026

Batstone D. J. and Keller J. (2003). Industrial applications of the IWA anaerobic digestion model No.1 (ADM1). *Water Science & Technology*, **47**, 199–206.

Batstone D. J., Keller J., Angelidaki I., Kalyuzhnyi S. V., Pavlostathis S. G., Rozzi A., Sanders W. T., Siegrist H. and Vavilin V. A. (2002). The IWA Anaerobic Digestion Model No 1 (ADM1). *Water Science & Technology*, **45**, 65–73, https://doi.org/10.2166/wst.2008.678

Batstone D. J., Keller J. and Steyer J. P. (2006). A review of ADM1 extensions, applications, and analysis: 2002–2005. *Water Science & Technology*, **54**, 1–10, https://doi.org/10.2166/wst.2006.520

Batstone D. J., Amerlinck Y., Ekama G., Goel R., Grau P., Johnson B., Kaya I., Steyer J. P., Tait S., Takacs I., Vanrolleghem P. A., Brouckaert C. J. and Volcke E. (2012). Towards a generalized physicochemical framework. *Water Science & Technology*, **66**, 1147–1161, https://doi.org/10.2166/wst.2012.300

Bhaskar P. and Bhosle N. (2006). Bacterial extracellular polymeric substances (EPS): A carrier of heavy metals in the marine food chain. *Environment International*, **32**, 1–8.

Blumensaat F. and Keller J. (2005). Modelling of two-stage anaerobic digestion using the IWA Anaerobic Digestion Model No. 1 (ADM1). *Water Research*, **39**, 171–83, https://doi.org/10.1016/j.watres.2004.07.024

Callander I. J. and Barford J. P. (1983a). Precipitation, chelation, and the availability of metals as nutrients in anaerobic digestion. II. Applications. *Biotechnology and Bioengineering*, **25**, 1959–1972, https://doi.org/10.1002/bit.260250806

Callander I. J. and Barford J. P. (1983b). Metals as Nutrients in Anaerobic Digestion. *Biotechnology and Bioengineering*, **25**, 1959–1972.

Chen Y., Cheng J. J. and Creamer K. S. (2008). Inhibition of anaerobic digestion process: A review. *Bioresource Technology*, **99**(10), 4044–4064, https://doi.org/10.1016/j.biortech.2007.01.057.

Choong Y. Y., Ismail N., Abdullah A. Z. and Yhaya M. F. (2016). Impacts of trace element supplementation on the performance of anaerobic digestion process: A critical review. *Bioresource Technology*, **209**, 369–379, https://doi.org/10.1016/j.biortech.2016.03.028

Copp J. B., Jeppsson U. and Rosen C. (2003). Towards an ASM1 – ADM1 State Variable Interface for Plant-Wide Wastewater Treatment Modelling. *Proceeding Water Environmental Federation*, 498–510, https://doi.org/10.2175/193864703784641207

d'Abzac P., Bordas F., van Hullebusch E., Lens P. N. L. and Guibaud G. (2010). Metal binding properties of extracellular polymeric substances extracted from anaerobic granular sludges. *Colloids Surfaces B Biointerfaces*, **80**, 161–168, https://doi.org/10.1016/j.colsurfb.2010.05.043

Daughney C. J. and Fein J. B. (1998). The Effect of Ionic Strength on the Adsorption of H+, Cd2+, Pb2+, and Cu2+ by Bacillus subtilis and Bacillus licheniformis: A Surface Complexation Model. *Journal of Colloid and Interface Science*, **198**, 53–77, https://doi.org/10.1006/jcis.1997.5266

Dezham P., Rosenblum E. and Jenkins D. (1988). Digester gas control using iron salts. *Journal -Water Pollution Control Federation*, **60**(4), 514–517.

Donoso-Bravo A., Bandara W. M. K. R. T. W., Satoh H. and Ruiz-Filippi G. (2013). Explicit temperature-based model for anaerobic digestion: Application in domestic wastewater treatment in a UASB reactor. *Bioresource Technology*, **133**, 437–442, https://doi.org/10.1016/j.biortech.2013.01.174

Droop M. R. (1983). 25 Years of Algal Growth Kinetics A Personal View. *Botanica Marina*, **26**, 99–112.

Ebigbo A., Phillips A., Gerlach R., Helmig R., Cunningham A. B., Class H. and Spangler L. H. (2012). Darcy-scale modeling of microbially induced carbonate mineral precipitation in sand columns. *Water Resources Research*, **48**(7).

England J. L. (2013). Statistical physics of self-replication. *Journal of Chemical Physics*, **139**, 121923, https://doi.org/10.1063/1.4818538

Federation W. E. (2014). Mineral nutrient requirements for high-rate methane fermentation of acetate at low In: SRTM. Takashima and R. E. Speece (eds), *Research Journal of the Water Pollution Control Federation*, **61**(11/12), http://www.jst 61, 1645–1650.

Federovich V., Lens P. and Kalyuzhnyi S. (2003). Extension of Anaerobic Digestion Model No. 1. Appl. *Biochemistry & Biotechnology*, **109**, 33–45, https://doi.org/10.1385/ABAB:109:1-3:33

Feng X. M., Karlsson A., Svensson B. H. and Bertilsson S. (2010). Impact of trace element addition on biogas production from food industrial waste – Linking process to microbial communities. *FEMS Microbiology Ecology*, **74**, 226–240, https://doi.org/10.1111/j.1574-6941.2010.00932.x

Fermoso F. G., Bartacek J., Jansen S. and Lens P. N. L. (2008). Metal supplementation to UASB bioreactors: From cell-metal interactions to full-scale application. *The Science of the Total Environment*, **407**, 3652–3667, https://doi.org/10.1016/j.scitotenv.2008.10.043

Fermoso F. G., Bartacek J., Jansen S. and Lens P. N. L. (2009). Metal supplementation to UASB bioreactors: From cell-metal interactions to full-scale application. *The Science of the Total Environment*, **407**, 3652–3667, https://doi.org/10.1016/j.scitotenv.2008.10.043

Fermoso F. G., Hullebusch E. D., Van Guibaud G., Collins G., Svensson B. H., Vink J. P. M., Esposito G. and Frunzo L. (2015). Fate of Trace Metals in Anaerobic Digestion. Trace metal microbiology. In: Biogas Science and Technology, A. Gübitz, A. Bauer, G. Bochmann, A. Gronauer and S. Weiss (eds), Springer, Berlin, https://doi.org/10.1007/978-3-319-21993-6

Finazzo C., Harmer J., Bauer C., Jaun B., Duin E. C., Mahlert F., Goenrich M., Thauer R. K., Van Doorslaer S. and Schweiger A. (2003). Coenzyme B induced coordination of coenzyme M via its thiol group to Ni(I) of F430 in active methyl-coenzyme M reductase. *Journal of the American Chemical Society*, **125**, 4988–4989, https://doi.org/10.1021/ja0344314

Flores-Alsina X., Solon K., Mbamba C. K., Tait S., Gernaey K. V., Jeppsson U. and Batstone D. J. (2016). Modelling phosphorus (P), sulfur (S) and iron (Fe) interactions for dynamic simulations of anaerobic digestion processes. *Water Research*, **95**, 370–382, https://doi.org/10.1016/j.watres.2016.03.012

Flynn S. L., Szymanowski J. E. and Fein J. B. (2014). Modeling bacterial metal toxicity using a surface complexation approach. *Chemical Geology*, **374**, 110–116.

Galí A., Benabdallah T., Astals S. and Mata-Alvarez J. (2009). Modified version of ADM1 model for agro-waste application. *Bioresource Technology*, **100**, 2783–2790, https://doi.org/10.1016/j.biortech.2008.12.052

Glass J. B. and Orphan V. J. (2012). Trace metal requirements for microbial enzymes involved in the production and consumption of methane and nitrous oxide. *Front Microbiology*, **3**, 1–20, https://doi.org/10.3389/fmicb.2012.00061

Gonzalez-Gil G. and Kleerebezem R. (1999). Effects of Nickel and Cobalt on Kinetics of Methanol Conversion by Methanogenic Sludge as Assessed by On-Line CH 4 Monitoring *Appl. Environmental Biology*, **65**, 1789–1793.

Gonzalez-Gil G., Jansen S., Zandvoort M. H. and Van Leeuwen H. P. (2003). Effect of yeast extract on speciation and bioavailability of nickel and cobalt in anaerobic bioreactors. *Biotechnology and Bioengineering*, **82**, 134–142, https://doi.org/10.1002/bit.10551

Gu Y., Zhang Y. and Zhou X. (2015). Effect of Ca(OH)2pretreatment on extruded rice straw anaerobic digestion. *Bioresource Technology*, **196**, 116–122.

Gustavsson J. (2012). Cobalt and Nickel Bioavailability for Biogas Formation. PhD thesis, University of Linkoping, Sweden.

Hanhoun M., Montastruc L., Azzaro-pantel C., Biscans B., Frèche M. and Pibouleau L. (2011). Temperature impact assessment on struvite solubility product: A thermodynamic modelling approach. *Chemical Engineering Journal*, **167**, 50–58, https://doi.org/10.1016/j.cej.2010.12.001

Hauduc H., Smith S., Szabo A., Murthy S. and Tak I. (2015). A dynamic physicochemical model for chemical phosphorus removal. *Water Research*, **73**, 157–170.

Henze M., Gujer W., Mino T., Matsuo T., Wentzel M. C., Marais G. V. R. and Van Loosdrecht M. C. M. (1999). Activated Sludge Model No.2d, ASM2d. *Water Science & Technology*, **39**, 165–182, https://doi.org/10.1016/S0273-1223(98)00829-4

Hickey R. F., Vanderwielen J. and Switzenbaum M. S. (1989). The effect of heavy metals on methane production and hydrogen and carbon monoxide levels during batch anaerobic sludge digestion. *Water Research*, **23**, 207–218, https://doi.org/10.1016/0043-1354(89)90045-6

Hille R., Van Foster T., Storey A. and Duncan J. (2004). Heavy metal precipitation by sulphide and bicarbonate: evaluating methods to predict anaerobic digester overflow performance. In: Mine Water 2004–Proceedings Int. Mine Water Assoc. Symp, A. P. Jarvis, B. A. Dudgeon and P. L. Younger (eds), **2**, 141–150.

Huang C., Lai J., Sun X., Li J., Shen J., Han W. and Wang L. (2016). Enhancing anaerobic digestion of waste activated sludge by the combined use of NaOH and Mg(OH)2: Performance evaluation and mechanism study. *Bioresource Technology*, **220**, 601–608.

Hudson R. J. M. (1998). Which aqueous species control the rates of trace metal uptake by aquatic biota? Observations and predictions of non-equilibrium effects. *The Science of the Total Environment*, **219**, 95–115, https://doi.org/10.1016/S0048-9697(98)00230-7

Jansen S. (2004). Speciation and bioavailability of cobalt and nickel in anaerobic wastewater treatment. PhD thesis, Leerstoelgroep Fysische Chemie en Kolloidkunde, Wageningen Univeristy, The Netherlands.

Jeen S. W., Amos R. T. and Blowes D. W. (2012). Modeling gas formation and mineral precipitation in a granular iron column. *Environmental Science & Technology*, **46** (12), 6742–6749.

Jiang B. (2006). The effect of trace elements on the metabolism of methanogenic consortia. PhD thesis, Wageningen University, The Netherlands.

Jimenez J., Latrille E., Harmand J., Robles A., Ferrer J., Gaida D., Wolf C., Mairet F., Bernard O., Alcaraz-Gonzalez V., Mendez-Acosta H., Zitomer D., Totzke D., Spanjers H., Jacobi F., Guwy A., Dinsdale R., Premier G., Mazhegrane S., Ruiz-Filippi G., Seco A., Ribeiro T., Pauss A. and Steyer J. P. (2015). Instrumentation and control of anaerobic digestion processes: A review and some research challenges. *Reviews Environmental Science Biotechnology*, **14**, 615–648, https://doi.org/10.1007/s11157-015-9382-6

Johnson B. R. and Shang Y. (2006). Applications and limitations of ADM 1 in municipal wastewater solids treatment. *Water Science & Technology*, **54**, 77–82, https://doi.org/10.2166/wst.2006.528

Kalyuzhnyi S. and Fedorovich V. (1997). Integrated mathematical model of UASB reactor for competition between sulphate reduction and methanogenesis. *Water Science & Technology*, **36**, 201–208, https://doi.org/10.1016/S0273-1223(97)00524-6

Kalyuzhnyi S. V. and Fedorovich V. V. (1998). Mathematical modelling of competition between sulphate reduction and methanogenesis in anaerobic reactors. *Bioresource Technology*, **65**, 227–242, https://doi.org/10.1016/S0960-8524(98)00019-4

Kalyuzhnyi S., Fedorovich V., Lens P. and Pol L. H. (1998). Mathematical modelling as a tool to study population dynamics between sulfate reducing and methanogenic bacteria. *Biodegradation*, **9**, 187–199.

Kauder J., Boes N., Pasel C. and Herbell J. D. (2007). Combining models ADM1 and ASM2d in a sequencing batch reactor simulation. *Chemical Engineering Technology*, **30**, 1100–1112, https://doi.org/10.1002/ceat.200700045

Kleerebezem R. and van Loosdrecht M. C. M. (2006). Critical analysis of some concepts proposed in ADM1. *Water Science & Technology*, **54**, 51, https://doi.org/10.2166/wst.2006.525

Knobel A. N. and Lewis A. E. (2002). A mathematical model of a high sulphate wastewater anaerobic treatment system. *Water Research*, **36**, 257–265, https://doi.org/10.1016/S0043-1354(01)00209-3

Koster W. and Van Leeuwen H. P. (2004). Physicochemical kinetics and transport at the biointerface: Setting the stage. In: *Iupac Series on Analytical and Physical Chemistry of Environmental Systems*, **9**, 1–14.

Kong X., Wei Y., Xu S., Liu J., Li H., Liu Y. and Yu S. (2016). Inhibiting excessive acidification using zero-valent iron in anaerobic digestion of food waste at high organic load rates. *Bioresource Technology*, **211**, 65–71, https://doi.org/10.1016/j.biortech.2016.03.078

Konhauser K. (2007). Introduction to geomicrobiology. *European Journal of Soil Science*, **58** (5), 1215–1216, https://doi.org/10.1111/j.1365-2389.2007.00943_4.x

Koutsoukos P., Amjad Z., Tomson M. B. and Nancollas G. H. (1980). Crystallization of calcium phosphates. A constant composition study. *Journal of the American Chemical Society*, **102**(5), 1553–1557.

Lawrence A. W. and McCarty P. L. (1965). The Role of Sulfide in Preventing Heavy Metal Toxicity in Anaerobic Treatment. *Journal Water Pollution Control Federation*, **37**, 392–406.

Lauwers J., Appels L., Thompson I. P., Degrève J., Impe J. F. and Van Dewil R. (2013). Mathematical modelling of anaerobic digestion of biomass and waste: Power and limitations. *Progress in Energy and Combustion Science*, **39**, 383–402, https://doi.org/10.1016/j.pecs.2013.03.003

Lin C.-Y. (1992). Effect of heavy metals on volatile fatty acid degradation in anaerobic digestion. *Water Research*, **26**, 177–183, https://doi.org/10.1016/0043-1354(92)90217-r

Lizarralde I., Fernández-Arévalo T., Brouckaert C., Vanrolleghem P., Ikumi D. S., Ekama G. A., Ayesa E. and Grau P. (2015). A new general methodology for incorporating physico-chemical transformations into multi-phase wastewater treatment process models. *Water Research*, **74**, 239–256, https://doi.org/10.1016/j.watres.2015.01.031

Loaec M., Olier R. and Guezennec J. (1997). uptake of lead, cadmium and zinc by bacterial exopolysaccharide. *Water Research*, **31**, 1171–1997.

Lopez-Vazquez C. M., Mithaiwala M., Moussa M. S., van Loosdrecht M. C. M. and Brdjanovic D. (2013). Coupling ASM3 and ADM1 for wastewater treatment process optimisation and biogas production in a developing country: Case-study Surat, India.

Journal Water, Sanitation Hygiene Development, **3**, 12, https://doi.org/10.2166/washdev.2013.017

MacConnell C. B. and Collins H. P. (2009). Utilization of re-processed anaerobically digested fiber from dairy manure as a container media substrate. *Acta Horticulturae*, **819**, 279–286.

Maharaj B. C., Mattei M. R., Frunzo L., van Hullebusch E. D. and Esposito G. (2018). ADM1 based mathematical model of trace element precipitation/dissolution in anaerobic digestion processes. *Bioresource Technology*, **267**, 666–676, https://doi.org/10.1016/j.biortech.2018.06.099

Malik A. (2004). Metal bioremediation through growing cells. *Environment International*, **30**, 261–278, https://doi.org/10.1016/j.envint.2003.08.001

Maurer M. and Boller M. (1999). Modelling of phosphorus precipitation in wastewater treatment plants with enhanced biological phosphorus removal. *Water Science & Technology*, **39**, 147–163, https://doi.org/10.1016/S0273-1223(98)00784-7

Maurer M., Abramovich D., Siegrist H. and Gujer W. (1999). Kinetics of biologically induced phosphorus precipitation in waste-water treatment. *Water Research*, **33**, 484–493, https://doi.org/10.1016/S0043-1354(98)00221-8

Mazumder T. K., Nishio N., Fukuzaki S. and Nagai S. (1987). Production of extracellular vitamin B-12 compounds from methanol by Methanosarcina barkeri. *Applied Microbiology and Biotechnology*, **26**, 511–516, https://doi.org/10.1007/BF00253023

Mbamba C. K., Batstone D. J., Flores-Alsina X. and Tait S. (2015a). A generalised chemical precipitation modelling approach in wastewater treatment applied to calcite. *Water Research*, **68**, 342–353.

Mbamba C. K., Tait S., Flores-Alsina X. and Batstone D. J. (2015b). A systematic study of multiple minerals precipitation modelling in wastewater treatment. *Water Research*, **85**, 359–370.

Morel F. and Morgan J. (1972). Numerical method for computing equilibriums in aqueous chemical systems. *Environmental Science & Technology*, **6**(1), 58–67.

Morse J. W. and Arakaki T. (1993). Adsorption and coprecipitation of divalent metals with mackinawite (FeS). *Geochimica et Cosmochimica Acta*, **57**(15), 3635–3640.

Mu H., Chen Y. and Xiao N. (2011). Effects of metal oxide nanoparticles (TiO2, Al2O3, SiO2and ZnO) on waste activated sludge anaerobic digestion. *Bioresource Technology*, **102**, 10305–10311.

Mudhoo A. and Kumar S. (2013). Effects of heavy metals as stress factors on anaerobic digestion processes and biogas production from biomass. *International Journal Environmental Science Technology*, **10**, 1383–1398, https://doi.org/10.1007/s13762-012-0167-y

Musvoto E. V., Wentzel M. C., Loewenthal R. E. and Ekama G. A. (2000a). Integrated chemical-physical processes modelling – I. Development of a kinetic-based model for mixed weak acid/base systems. *Water Research*, **34**, 1857–1867, https://doi.org/10.1016/S0043-1354(99)00334-6

Musvoto E. V, Wentzel M. C. M. and Ekama G. a. M. (2000b). Integrated Chemical Physical Processes Modelling -II. Simulating Aeration Treatment of Anaerobic Digester Supernatants. *Water Research*, **34**, 1868–1880.

Nopens I., Batstone D. J., Copp J. B., Jeppsson U., Volcke E., Alex J. and Vanrolleghem P. a. (2009). An ASM/ADM model interface for dynamic plant-wide simulation. *Water Research*, **43**, 1913–1923, https://doi.org/10.1016/j.watres.2009.01.012

Ohlinger K. N., Young T. M. and Schroeder E. D. (1998). Predicting struvite formation in digestion. *Water Research*, **32**, 3607–3614, https://doi.org/10.1016/S0043-1354(98)00123-7

Oleszkiewicz J. A. and Sharma V. K. (1990). Stimulation and inhibition of anaerobic processes by heavy metals-A review. *Biology Wastes*, **31**, 45–67, https://doi.org/10.1016/0269-7483(90)90043-R

Oude Elferink S. J. W. H., Visser A., Hulshoff Pol L. W. and Stams A. J. M. (1994). Sulfate reduction in methanogenic bioreactors. *FEMS Microbiology Reviews*, **15**, 119–136, https://doi.org/10.1016/0168-6445(94)90108-2

Papirio S., Frunzo L., Mattei M. R. and Ferraro A. (2017). Sustainable Heavy Metal Remediation, Springer, Berlin, https://doi.org/10.1007/978-3-319-61146-4

Parker W. J. and Wu G.-H. (2006). Modifying ADM1 to include formation and emission of odourants. *Water Science & Technology*, **54**, 111–117, https://doi.org/10.2166/wst.2006.532

Paulo L. M., Stams A. J. M. and Sousa D. Z. (2015). Methanogens, sulphate and heavy metals: A complex system. *Reviwes Environmetal Science Biology*, **14**, 537–553.

Peiris B. R. H., Rathnasiri P. G., Johansen J. E., Kuhn A. and Bakke R. (2006). ADM1 simulations of hydrogen production. *Water Science & Technology*, **53**, 129–137, https://doi.org/10.2166/wst.2006.243

Peng S. and Colosi L. M. (2016). Anaerobic digestion of algae biomass to produce energy during wastewater treatment. *Water Environment Research*, **88**(1), 29–39.

Poinapen J. and Ekama G. A. (2010). Biological sulphate reduction with primary sewage sludge in an upflow anaerobic sludge bed reactor - Part 6: Development of a kinetic model for BSR. *Water Sa*, **36**(3), 203–214.

Preis W. and Gamsjäger H. (2001). Thermodynamic investigation of phase equilibria in metal carbonate–water–carbon dioxide systems. *Monatshefte fuer Chemie/Chemical Monthly*, **132**(11), 1327–1346.

Qiao L. and Ho G. (1996). The effect of clay amendment on speciation of heavy metals in sewage sludge. *Water Science and Technology*, **34**(7-8), 413–420.

Rahaman M. S., Mavinic D. S., Meikleham A. and Ellis N. (2014). Modelling phosphorus removal and recovery from anaerobic digester supernatant through struvite crystallization in a fluidized bed reactor. *Water Research*, **51**, 1–10, https://doi.org/10.1016/j.watres.2013.11.048

Reichert P. (1994). *AQUASIM* – A tool for simulation and data analysis of aquatic systems. *Water Science & Technology*, **30**(2), 21–30.

Ristow N. E., Whittington-Jones K., Corbett C., Rose P. and Hansford G. S. (2002). Modelling of a recycling sludge bed reactor using AQUASIM (vol 27, pg 445, 2001). *Water Sa*, **28**, 111–120.

Rittmann B. E., Banaszak J. E., VanBriesen J. M. and Reed D. T. (2002). Mathematical modelling of precipitation and dissolution reactions in microbiological systems. *Biodegradation*, **13**, 239–250, https://doi.org/10.1023/A:1021225321263

Romero-güiza M. S., Vila J., Mata-alvarez J., Chimenos J. M. and Astals S. (2016). The role of additives on anaerobic digestion: A review. *Renewable and Sustainable Energy Reviews*, **58**, 1486–1499, https://doi.org/10.1016/j.rser.2015.12.094

Rosen C., Vrecko D., Gernaey K. V., Pons M. N. and Jeppsson U. (2006). Implementing ADM1 for plant-wide benchmark simulations in Matlab/Simulink. *Water Science & Technology*, **54**, 11, https://doi.org/10.2166/wst.2006.521

Roussel J. (2012). Metal behaviour in anaerobic sludge digesters supplemented with trace nutrients. PhD Thesis, Univ. Birmingham, United Kingdom.

Roussel J. and Carliell-Marquet C. (2016). Significance of vivianite precipitation on the mobility of iron in anaerobically digested sludge. *Frontiers in Environmental Science*, **4**, 60.

Schwarz A. O. and Rittmann B. E. (2007). A biogeochemical framework for metal detoxification in sulfidic systems. *Biodegradation*, **18**, 675–692, https://doi.org/10.1007/s10532-007-9101-2

Scott W. D., Wrigley T. J., Webb K. M. and Science E. (1991). A computer model of struvite solution chemistry. *Talanta*, **38**, 889–895.

Shakeri S., Gustavsson J., Svensson B. H. and Skyllberg U. (2012). Sulfur K-edge XANES and acid volatile sulfide analyses of changes in chemical speciation of S and Fe during sequential extraction of trace metals in anoxic sludge from biogas reactors. *Talanta*, **89**, 470–477, https://doi.org/10.1016/j.talanta.2011.12.065

Shaojun Z. and Mucci A. (1993). Calcite precipitation in seawater using a constant addition technique: A new overall reaction kinetic expression. *Geochimica et Cosmochimica Acta*, **57**(7), 1409–1417.

Smith S., Takács I., Murthy S., Daigger G. T. and Szabó A. (2008). Phosphate Complexation Model and Its Implications for Chemical Phosphorus Removal. *Water Environment Research*, **80**, 428–438, https://doi.org/10.2175/106143008X268443

Solon K. (2015). IWA Anaerobic Digestion Model No. 1 extended with Phosphorus and Sulfur Literature Review, Division of Industrial Electrical Engineering and Automation Faculty of Engineering, Lund University, 1–16.

Solon K., Flores-Alsina X., Mbamba C. K., Volcke E. I. P., Tait S., Batstone D., Gernaey K. V. and Jeppsson U. (2015). Effects of ionic strength and ion pairing on (plant-wide) modelling of anaerobic digestion. *Water Research*, **70**, 235–245, https://doi.org/10.1016/j.watres.2014.11.035

Stumm W. and Morgan J. J. (1996). Aquatic Chemistry, 3rd ed. John Wiley and Sons, Inc, New York.

Stupperich E. and Kräutler B. (1988). Pseudo vitamin B12 or 5-hydroxybenzimidazolyl-cobamide are the corrinoids found in methanogenic bacteria. *Archives of Microbiology*, **149**, 268–271, https://doi.org/10.1007/BF00422016

Sunda W. G. and Huntsman S. A. (1998). Interactions among Cu2+, Zn2+, and Mn2+ in controlling cellular Mn, Zn, and growth rate in the coastal alga Chlamydomonas. *Limnol. Oceanogr*, **43**, 1055–1064, https://doi.org/10.4319/lo.1998.43.6.1055

Szabó A., Takács I., Murthy S., Daigger G. T., Licskó I. and Smith S. (2008). Significance of Design and Operational Variables in Chemical Phosphorus Removal. *Water Environment Research*, **80**, 407–416, https://doi.org/10.2175/106143008X268498

Tait S., Clarke W. P., Keller J. and Batstone D. J. (2009). Removal of sulfate from high-strength wastewater by crystallisation. *Water Research*, **43**, 762–772, https://doi.org/10.1016/j.watres.2008.11.008

Thanh P., Ketheesan B., Zhou Y. and Stuckey D. C. (2015). Trace metal speciation and bioavailability in anaerobic digestion: A review. *Biotechnology Advances*, **34**, 122–136, https://doi.org/10.1016/j.biotechadv.2015.12.006

Thauer R.K. (1998). Biochemistry of methanogenesis: A tribute to marjory stephenson: 1998 marjory stephenson prize lecture. *Microbiology*, **144**(9), 2377–2406.

Uemura S. (2010). Mineral Requirements for Mesophilic and Thermophilic Anaerobic Digestion of Organic Solid Waste. *International Journal of Environmental Research*, **4**, 33–40.

Uludag-Demirer S. and Othman M. (2009). Removal of ammonium and phosphate from the supernatant of anaerobically digested waste activated sludge by chemical precipitation. *Bioresource technology*, **100**(13), 3236–3244.

Van Briesen J. M. and Rittmann B. E. (1999). Modeling speciation effects on biodegradation in mixed metal/chelate systems. *Biodegradation*, **10**(5), 315–330.

van Hullebusch E. D., Guibaud G., Simon S., Lenz M., Shakeri Yekta S., Fermoso F. G., Jain R., Duester L., Roussel J., Guillon E., Skyllberg U., Almeida C. M. R., Pechaud Y., Garuti M., Frunzo L., Esposito G., Carliell-Marquet C., Ortner M. and Collins G. (2016). Methodological approaches for fractionation and speciation to estimate trace element bioavailability in engineered anaerobic digestion ecosystems: An overview. *Critical. Reviews Environmental Science and Technology*, **46**, 1324–1366, https://doi.org/10.1080/10643389.2016.1235943

Van Langerak E. P. A., Beekmans M. M. H., Beun J. J., Hamelers H. V. M. and Lettinga G. (1999). Influence of phosphate and iron on the extent of calcium carbonate precipitation during anaerobic digestion. *Journal of Chemical Technology & Biotechnology: International Research in Process, Environmental & Clean Technology*, **74**(11), 1030–1036.

Van Rensburg P., Musvoto E. V., Wentzel M. C. and Ekama G. A. (2003). Modelling multiple mineral precipitation in anaerobic digester liquor. *Water Research*, **37**, 3087–3097, https://doi.org/10.1016/S0043-1354(03)00173-8

Vavilin V. A., Vasiliev V. B., Rytov S. V. and Ponomarev A. V. (1995). Modelling ammonia and hydrogen sulfide inhibition in anaerobic digestion. *Water Research*, **29**, 827–835, https://doi.org/10.1016/0043-1354(94)00200-Q

Wang R., Li Y., Chen W., Zou J. and Chen Y. (2016). Phosphate release involving PAOs activity during anaerobic fermentation of EBPR sludge and the extension of ADM1. *Chemical Engineering Journal*, **287**, 436–447, https://doi.org/10.1016/j.cej.2015.10.110

Warren L. A. and Haack E. A. (2001). Biogeochemical controls on metal behaviour in freshwater environments. *Earth-Science Review*, **54**, 261–320, https://doi.org/10.1016/S0012-8252(01)00032-0

Willet A. I. and Rittmann B. E. (2003). Slow complexation kinetics for ferric iron and EDTA complexes make EDTA non-biodegradable. *Biodegradation*, **14**, 105–121, https://doi.org/10.1023/A:1024074329955

Worms I., Simon D. F., Hassler C. S. and Wilkinson K. J. (2006). Bioavailability of trace metals to aquatic microorganisms: Importance of chemical, biological and physical processes on biouptake. *Biochimie*, **88**, 1721–1731, https://doi.org/10.1016/j.biochi.2006.09.008

Wrigley T. J., Scoit W. D. and Webb K. M. (1992). An improved computer model of struvite. *Talanta*, **39**, 1597–1603.

Xu F., Li Y. and Wang Z. W. (2015). Mathematical modelling of solid-state anaerobic digestion. *Progress in Energy and Combustion Science*, **51**, 49–66, https://doi.org/10.1016/j.pecs.2015.09.001

Ye Z. L., Chen S. H., Wang S. M., Lin L. F., Yan Y. J., Zhang Z. J. and Chen J. S. (2010). Phosphorus recovery from synthetic swine wastewater by chemical precipitation using response surface methodology. *Journal of Hazardous Materials*, **176**(1-3), 1083–1088.

Yekta S. S., Lindmark A., Skyllberg U., Danielsson Å. and Svensson B. H. (2014a). Importance of reduced sulfur for the equilibrium chemistry and kinetics of Fe(II), Co (II) and Ni(II) supplemented to semi-continuous stirred tank biogas reactors fed with stillage. *Journal of Hazardous Materials*, **269**, 83–88, https://doi.org/10.1016/j.jhazmat.2014.01.051

Yekta S. S., Skyllberg U., Danielsson Å., Björn A. and Svensson B. H. (2016). Chemical speciation of sulfur and metals in biogas reactors—Implications for cobalt and nickel bio-uptake processes. *Journal of Hazardous Materials*, **324**, 110–116, https://doi.org/10.1016/j.jhazmat.2015.12.058

Yekta S. S., Svensson B. H., Björn A. and Skyllberg U. (2014b). Thermodynamic modelling of iron and trace metal solubility and speciation under sulfidic and ferruginous conditions in full scale continuous stirred tank biogas reactors. *Applied Geochemistry*, **47**, 61–73, https://doi.org/10.1016/j.apgeochem.2014.05.001

Zaher U. and Chen S. (2006). Interfacing the IWA Anaerobic Digestion Model No.1 (ADM1) with Manure and Solid Waste Characteristics. *Proceeding Water Environmental Federation*, **2006**(9), 3162–3175, https://doi.org/10.2175/193864706783751726

Zaher U., Grau P., Benedetti L., Ayesa E. and Vanrolleghem P. (2007). Transformers for interfacing anaerobic digestion models to pre- and post-treatment processes in a plant-wide modelling context. *Environmental Modelling Software*, **22**, 40–58, https://doi.org/10.1016/j.envsoft.2005.11.002

Zandvoort B. M. H., Hullebusch E. D. Van, Fermoso F. G. and Lens P. N. L. (2006). Trace Metals in Anaerobic Granular Sludge Reactors: Bioavailability and Dosing Strategies. *Engineering Life Science*, **6**, 293–301, https://doi.org/10.1002/elsc.200620129

Zhang T., Bowers K. E., Harrison J. H. and Chen S. (2010). Releasing phosphorus from calcium for struvite fertilizer production from anaerobically digested dairy effluent. *Water Environment Research*, **82**(1), 34–42.

Zhang W., Zhang L. and Li A. (2015). Enhanced anaerobic digestion of food waste by trace metal elements supplementation and reduced metals dosage by green chelating agent [S, S]-EDDS via improving metals bioavailability. *Water Research*, **84**, 266–277, https://doi.org/10.1016/j.watres.2015.07.010

Zhang Y., Piccard S. and Zhou W. (2015). Improved ADM1 model for anaerobic digestion process considering physico-chemical reactions. *Bioresource Technology*, **196**, 279–289, https://doi.org/10.1016/j.biortech.2015.07.065

Zhao W. E. and Yang H. (2014). Statistical Methods in Drug Combination Studies, CRC Press, Boca Raton, FL.

APPENDIX

Notation

$K_{A/B,H2S}$	Acid-base kinetic coefficient (m^3 $kmol^{-1}$ d^{-1})
$K_{H,H2S}$	Henry's law coefficient ($kmol^{-3}$ bar^{-1})
$K_{I,H2S}$	Inhibition coefficient by undissociated H_2S (kmol m^{-3})
K_{100}	Concentration of H_2S or pH at which the uptake rate is decreased 100 times (kmol m^{-3})
K_2	Concentration of H_2S or pH at which the uptake rate is decreased 2 times (kmol m^{-3})
$K_{a,H2S}$	Acid-base kinetic coefficient (m^3 $kmol^{-1}$)
$k_{dec,i}$	First order decay rate of species i (d^{-1})
k_la	Gas-liquid mass-transfer coefficient (d^{-1})
$k_{m,i}$	Monod maximum specific uptake rate (d^{-1})
k_{p2}	Competitive product inhibition coefficient (kg m^{-3})
$K_{S,j}$	Half saturation value (kg COD_Sm^{-3})
$K_{S_{SO4}}$	Half saturation value for sulfate (kg SO_4 m^{-3})
$P_{gas,H2S}$	Hydrogen sulfide partial pressure (bar)
S_j	Concentration of soluble organic components (kg COD m^{-3})
X_i	Concentration of particulate component i (kg COD m^{-3})
I_{pH}	pH inhibition function
I_{H_2s}	Sulfide inhibition function
$\rho_{A/B}$	Acid-base kinetic rate (kmol m^{-3} d^{-1})
ρ_{gas}	Liquid-gas kinetic gas transfer rate (kmol m^{-3} d^{-1})
$\rho_{decay,i}$	Kinetic rate of bacterial decay (kg COD m^{-3} d^{-1})
$\rho_{growth,i}$	Kinetic rate of microbial growth (kg COD m^{-3} d^{-1})